Electronic Supplementary Information (ESI) for

**Heck reaction between free base 2-Br-porphyrin and vinyl-ferrocene derivatives.
Electrochemical and spectroscopic characterisation of β-functionalized *alpha* and *trans*-vinyl-ferrocene porphyrin derivatives. A comparative study**

Miriam Demingo,[a] Angelo Lembo,*[a] Greta Petrella [a], Lorenzo Gontrani [a], Francesca Limosani [b,a], Giorgio Arrigoni[b], Marilena Carbone [a], Daniel O. Cicero[a] and Pietro Tagliatesta [a]

[a] Department of Chemical Science and Technologies, University of Rome "Tor Vergata", Via della Ricerca Scientifica 1, 00133 Rome

* Corresponding author e-mail: angelo.lembo@uniroma2.it

[b] Fusion and Technologies for Nuclear Safety and Security Department, Enea Casaccia Research Centre, Via Anguillarese, 301, 00123 S. Maria Di Galeria (Rome), Italy

[c] Department of Biomedical Sciences, University of Padova, Padova, Italy; Proteomics Center, University of Padova and Azienda Ospedaliera di Padova, Italy.

Tables of Contents

S1. Experimental section

S1.1.   Synthesis of vinylferrocene (compound 1)_Reaction scheme

The reaction scheme for the synthesis of vinylferrocene, following the procedure described in the "synthetic procedure", is reported below.
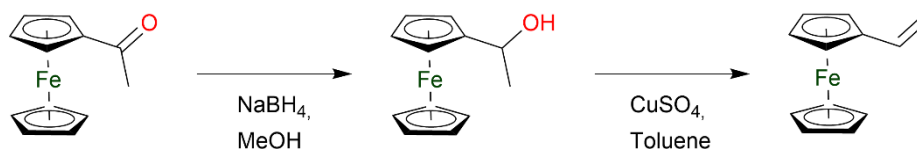
Scheme S 1 Reaction scheme for the synthesis of vinylferrocene

S1.2.   Synthesis of 4-ferrocenylstyrene (compound 2)_Reaction scheme

The reaction scheme for the synthesis of vinylferrocene following the procedure described in the "synthetic procedure" is reported below.
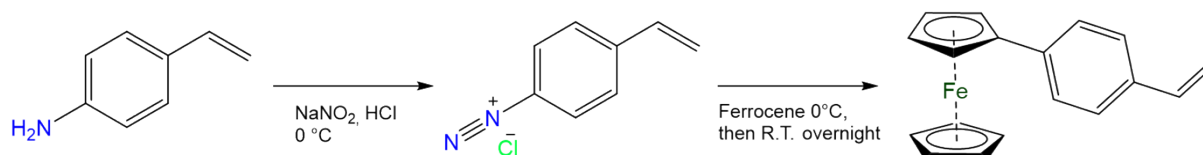
Scheme S 2 Reaction scheme for the synthesis of 4-ferrocenylstyrene

S2. Characterisation data

S2.1. Characterisation data for compound 1 (vinylferrocene)
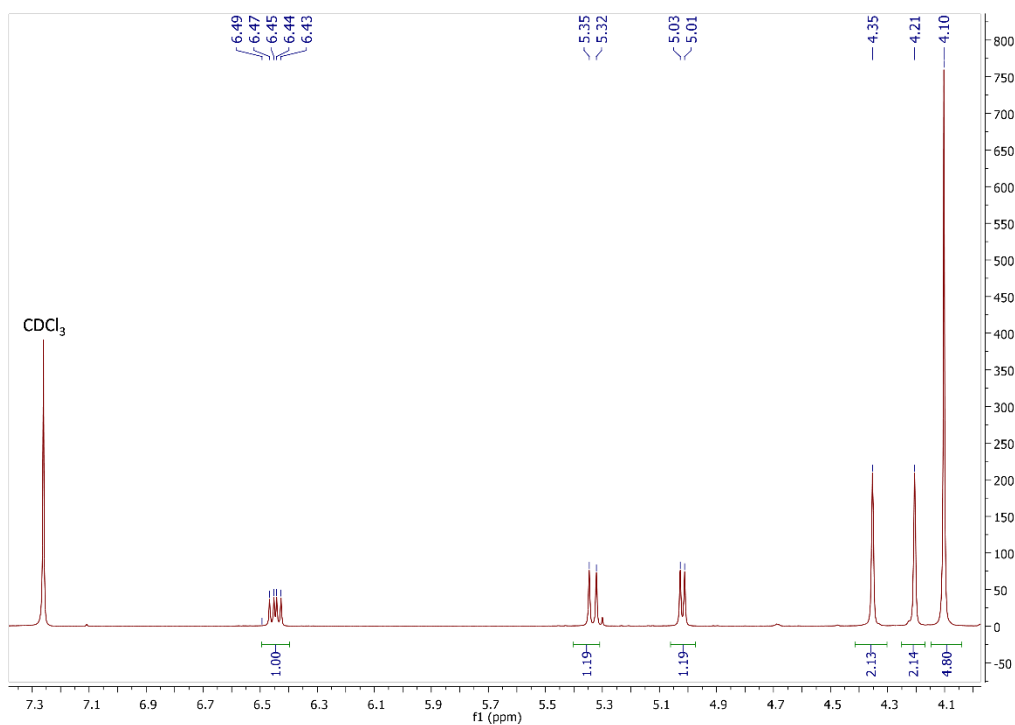
Fig. S 1 ^{1}H-NMR (700 MHz, CDCl$_3$) of compound **1**, vinylferrocene.
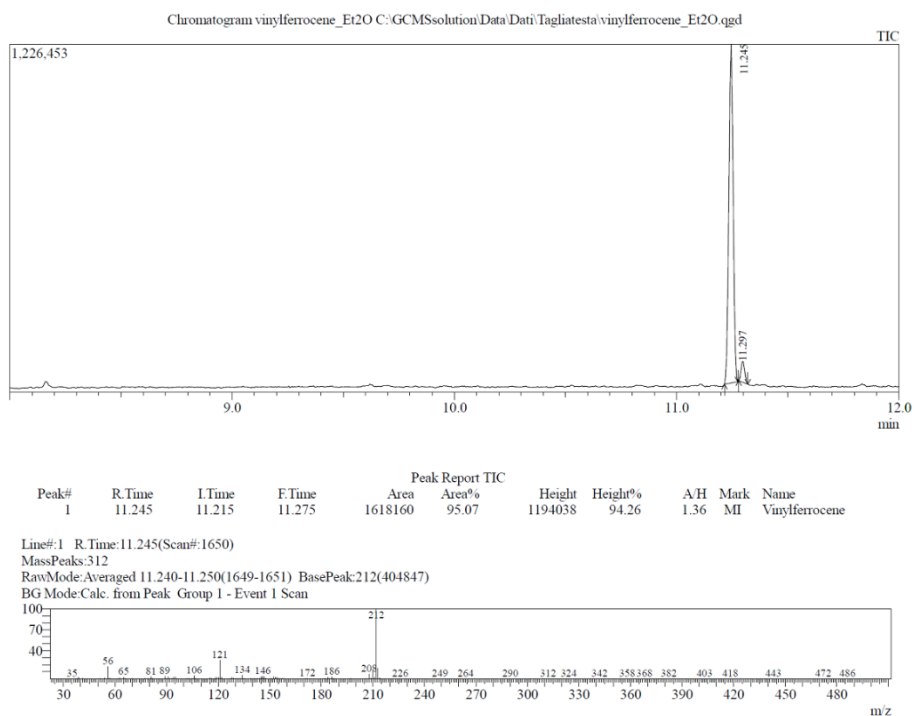
Fig. S 2 GC-MS characterisation of compound **1** (vinylferrocene). Chromatogram (upper part) and mass spectrum (lower part).

Characterisation data for compound 2 (4-ferrocenylstyrene)
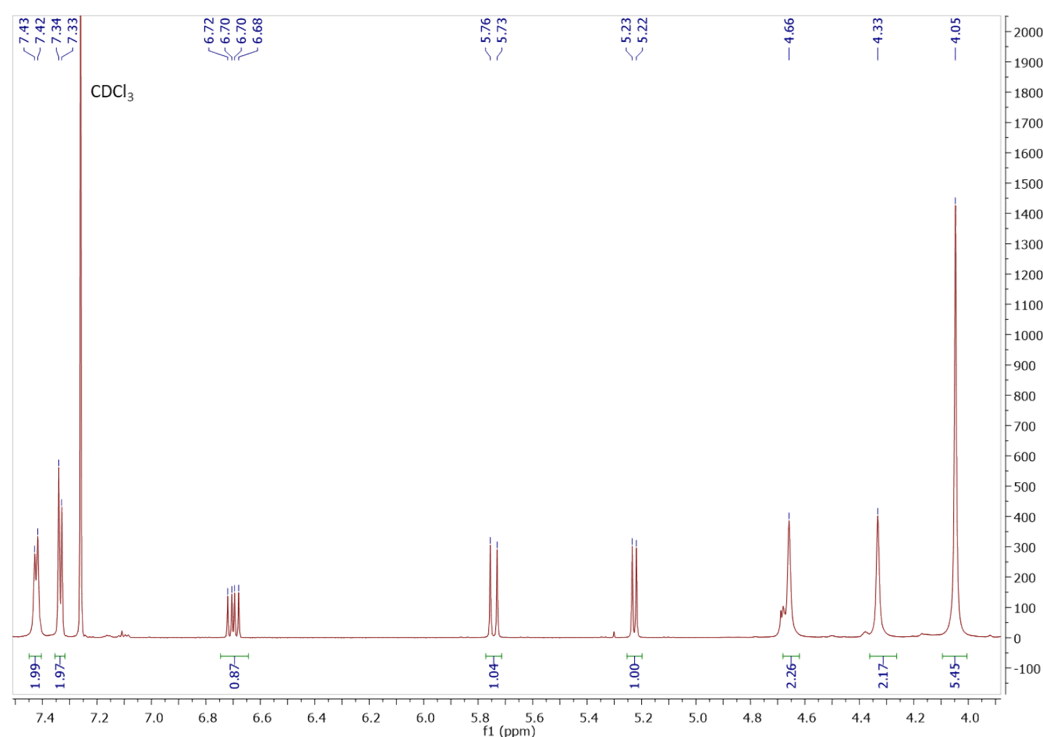
*Fig. S 3 ^{1}H-NMR (700 MHz, CDCl$_3$) of compound **2**, 4-Ferrocenylstyrene.*
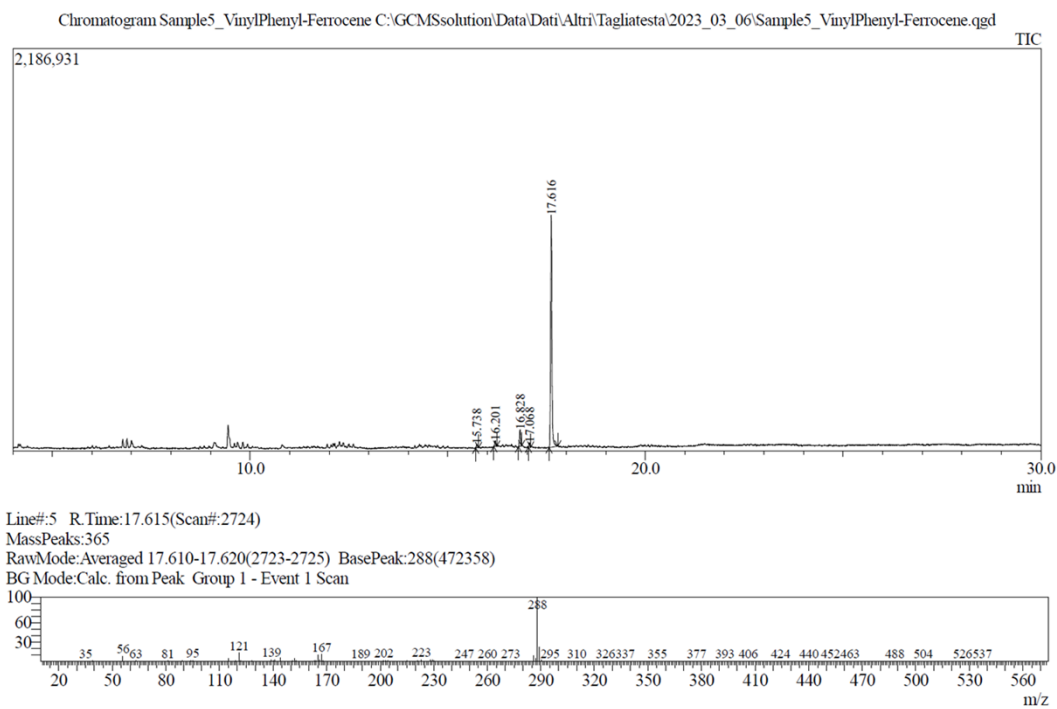
*Fig. S 4 GC-MS characterisation of compound **2** (4-ferrocenylstyrene). Chromatogram (upper part) and mass spectrum (lower part).*

Characterisation data for compound 4 (2-Br-5,10,15,20-tetraphenylporphyrin)
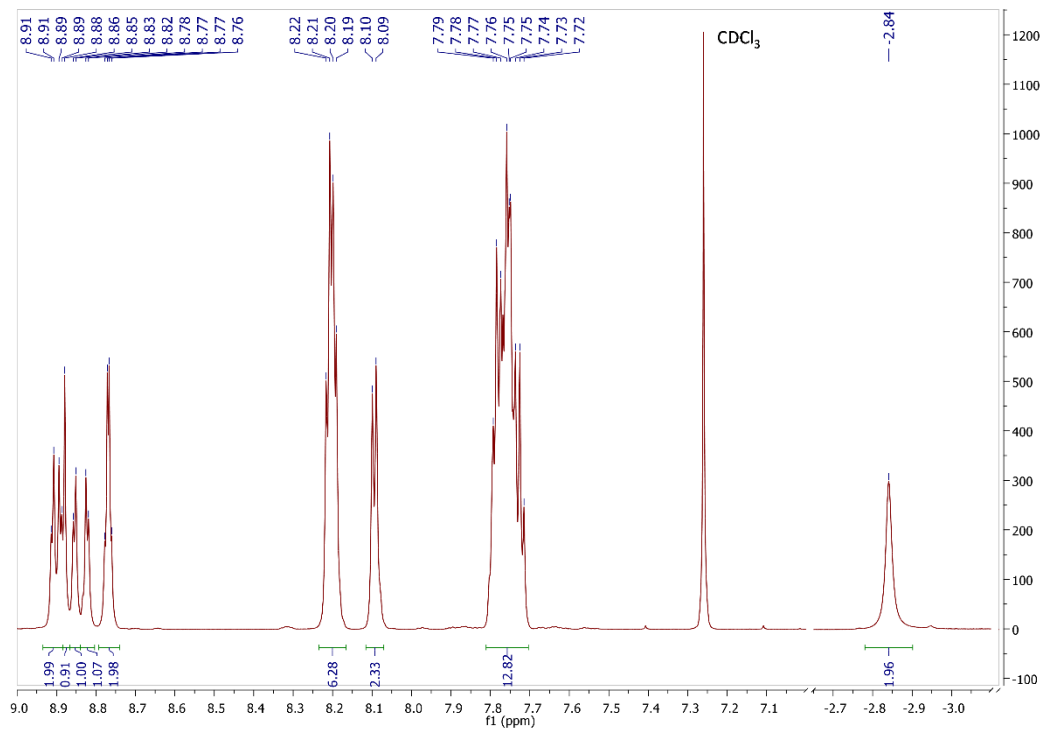
Fig. S 5 ^{1}H-NMR (700 MHz, CDCl$_3$) of compound **4**, 2-Br-5,10,15,20-tetraphenylporphyrin (2-Br-H$_2$TPP).
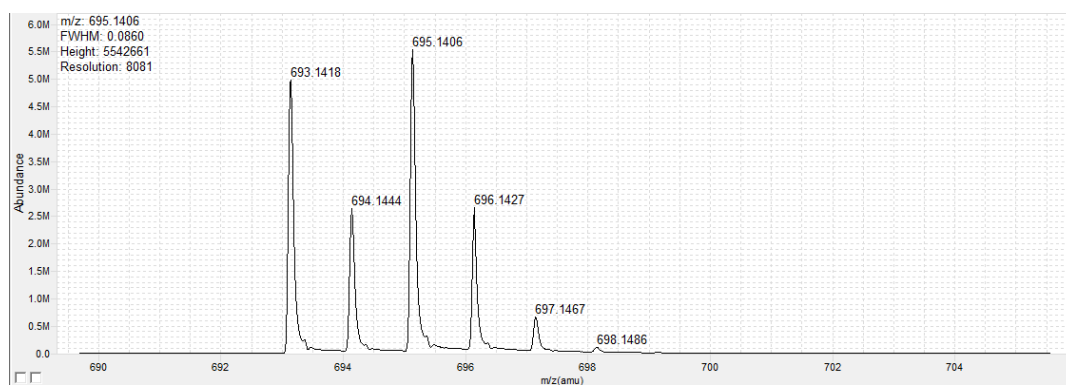
Fig. S 6 ESI HR-MS of compound **4**, 2-Br-5,10,15,20-tetraphenylporphyrin (2-Br-H$_2$TPP).

S2.4. Characterisation data for compound 5t (E) 2-(ferrocenyl)vinyl-5,10,15,20-tetraphenylporphyrin (*trans*-isomer)
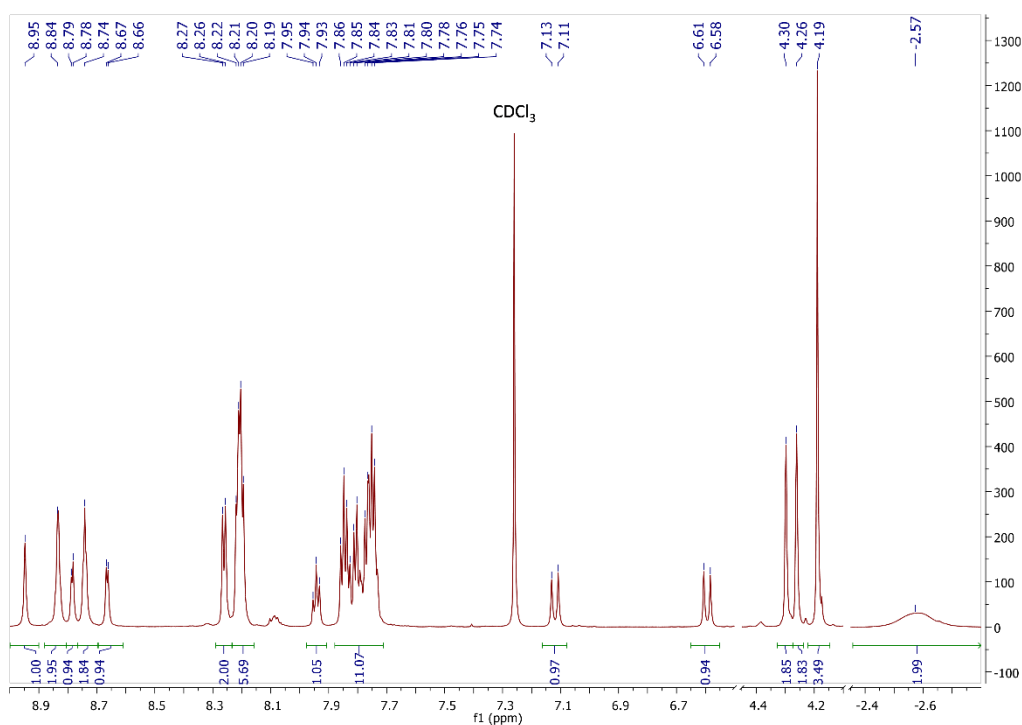
*Fig. S 7 ¹H-NMR (700 MHz, CDCl₃) of compound **5t**, (E) 2-(ferrocenyl)vinyl-5,10,15,20-tetraphenylporphyrin (trans-isomer).*
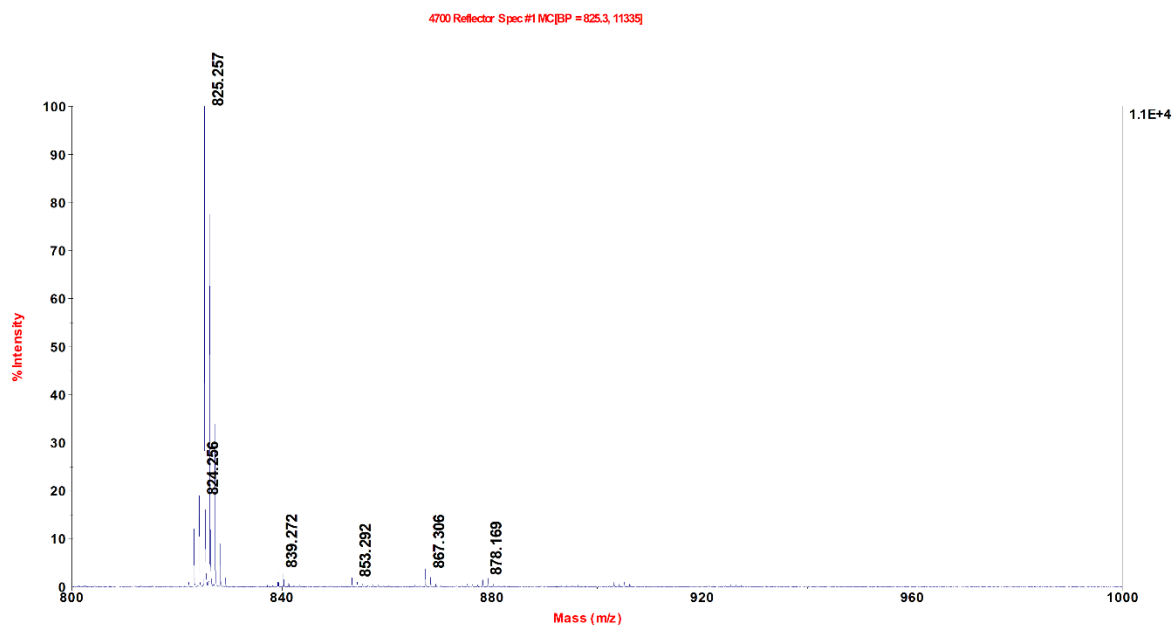
*Fig. S 8 MALDI HR-MS spectrum (full view) of compound **5t**, (E) 2-(ferrocenyl)vinyl-5,10,15,20-tetraphenylporphyrin (trans-isomer).*

110
100   2
90   0 profile: 823.2740427,6.36
80   1 profile: 824.2850882,3.86
70   3   2 profile: 825.2685597,101.15
60   3 profile: 826.2704139,65.01
50   4 profile: 827.2814594,20.53
40   5 profile: 828.2741223,4.46
30
20   4
10   0   1   5
0
     824   826   828   830
              m\z

relative abundance

4700 Reflector Spec #1 MC[BP = 825.3, 11335]

100   825.257   1.1E+4
90
80
70
60
50
40
30
20   823.291   824.266   827.37603
10
0
822.27002   823.97202   825.67402   827.37603   829.07803   830.78003
                        Mass (m/z)

%Intensity
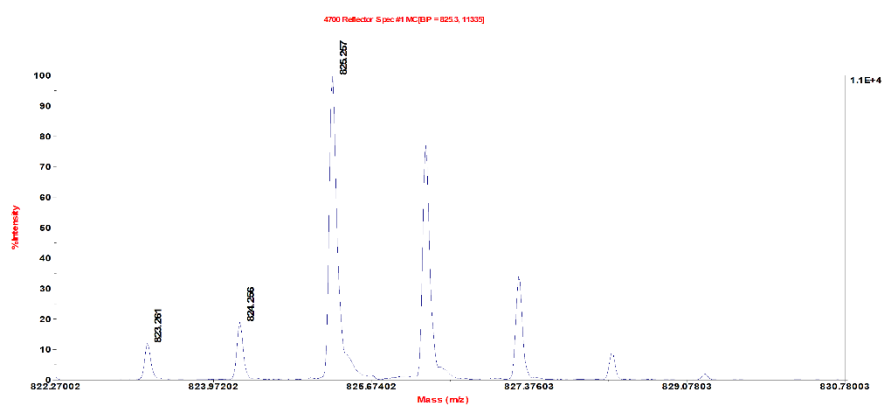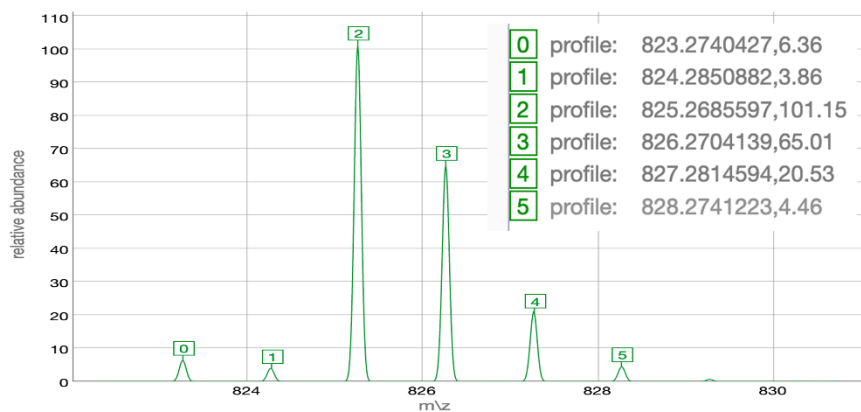
*Fig. S 9 MALDI HR-MS spectrum (molecular peak) of compound **5t**, (E) 2-(ferrocenyl)vinyl-5,10,15,20-tetraphenylporphyrin (trans-isomer). Theoretical (upper) and experimental (lower).*

9

S2.5. Characterisation data for compound 5α (α) 2-(ferrocenyl)vinyl-5,10,15,20-tetraphenylporphyrin (*alpha*-isomer)
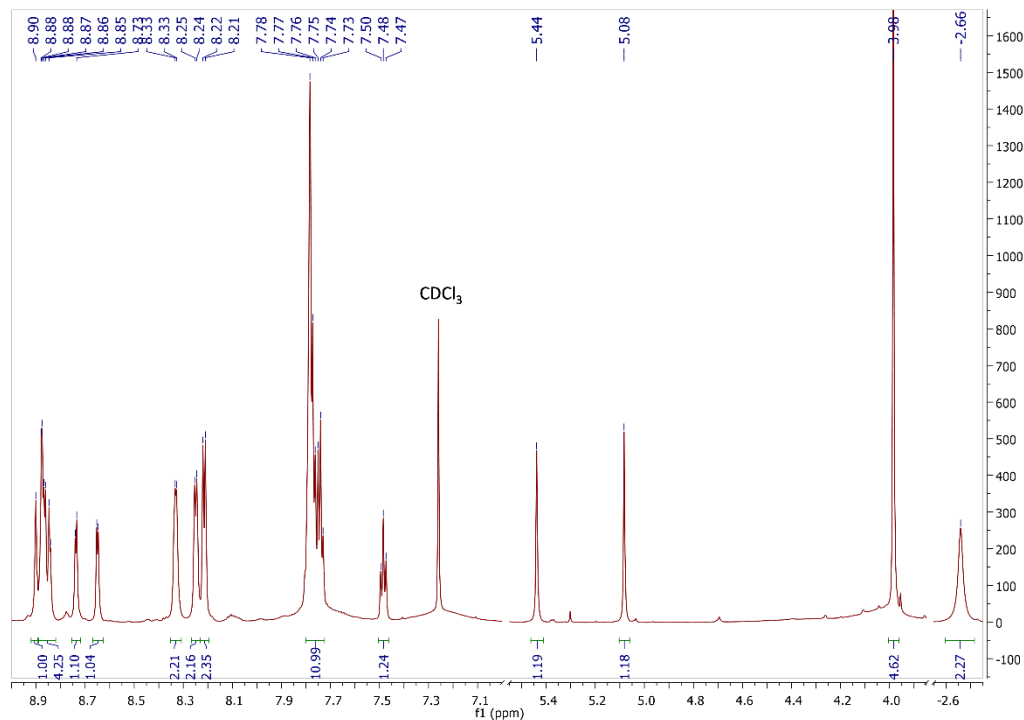
*Fig. S 10 ¹H-NMR (700 MHz, CDCl₃) of compound **5α**, (α) 2-(ferrocenyl)vinyl-5,10,15,20-tetraphenylporphyrin (alpha-isomer).*
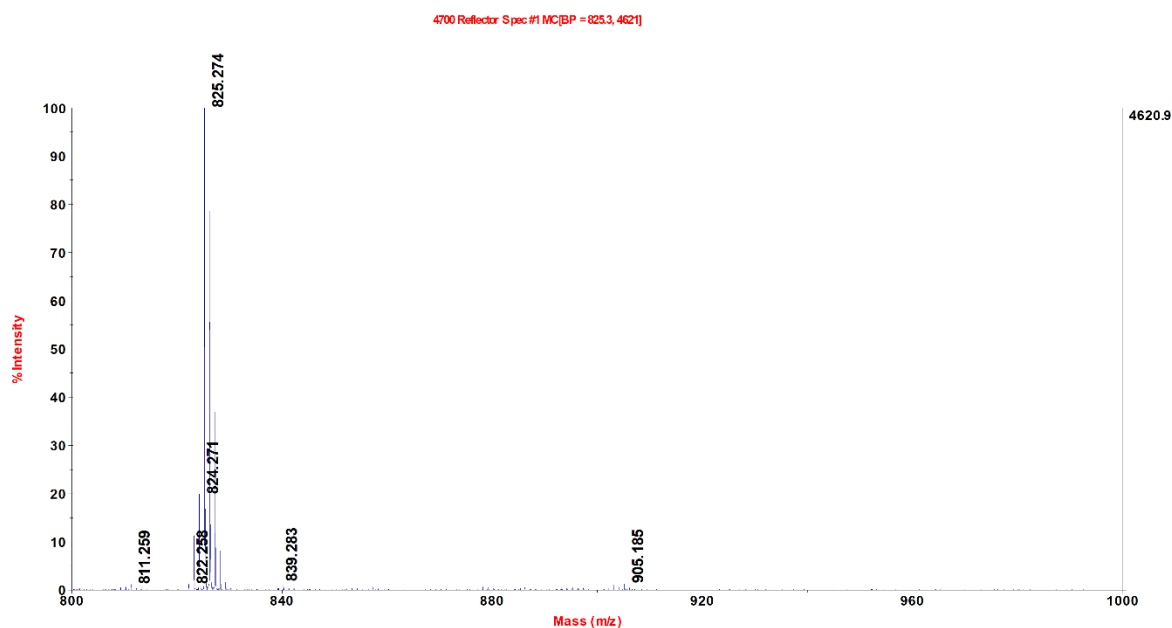
*Fig. S 11 MALDI HR-MS spectrum (full view) of compound **5α**, (α) 2-(ferrocenyl)vinyl-5,10,15,20-tetraphenylporphyrin (alpha-isomer).*

0	profile:	823.2740427,6.36
1	profile:	824.2850882,3.86
2	profile:	825.2685597,101.15
3	profile:	826.2704139,65.01
4	profile:	827.2814594,20.53
5	profile:	828.2741223,4.46
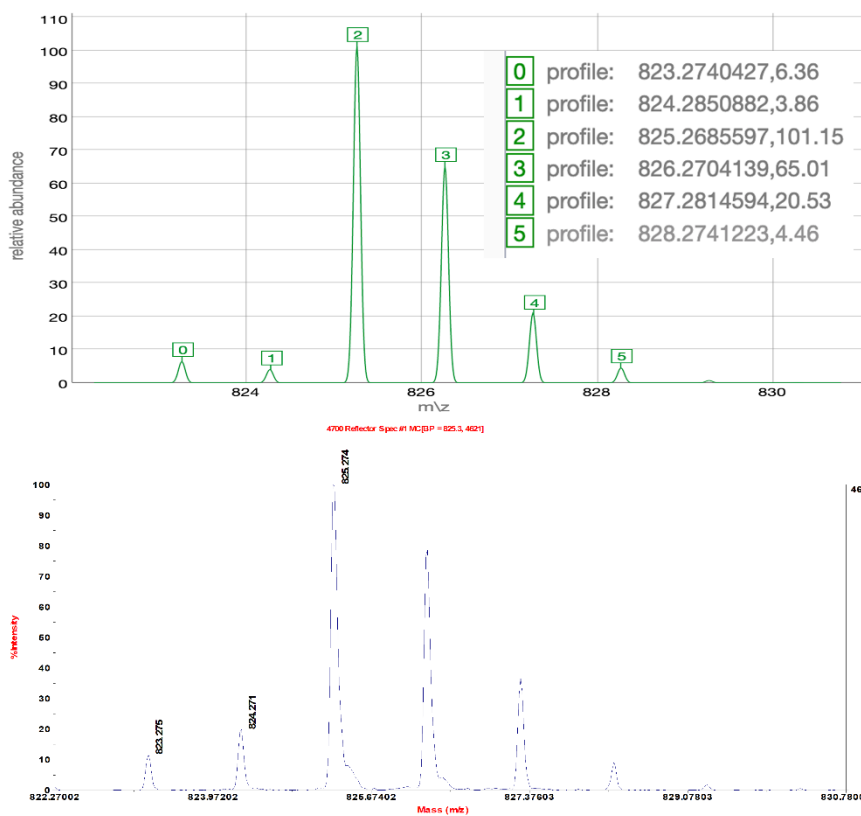
*Fig. S 12 MALDI HR-MS spectrum (molecular peak) of compound **5α,** (α) 2-(ferrocenyl)vinyl-5,10,15,20-tetraphenylporphyrin (trans-isomer). Theoretical (upper) and experimental (lower).*

*Fig. S 13 ^{1}H-NMR (700 MHz, CDCl$_3$) of compound **6t**, (E) 2-(4'-ferrocenylstyryl)-5,10,15,20-tetraphenylporphyrin (trans-isomer).*
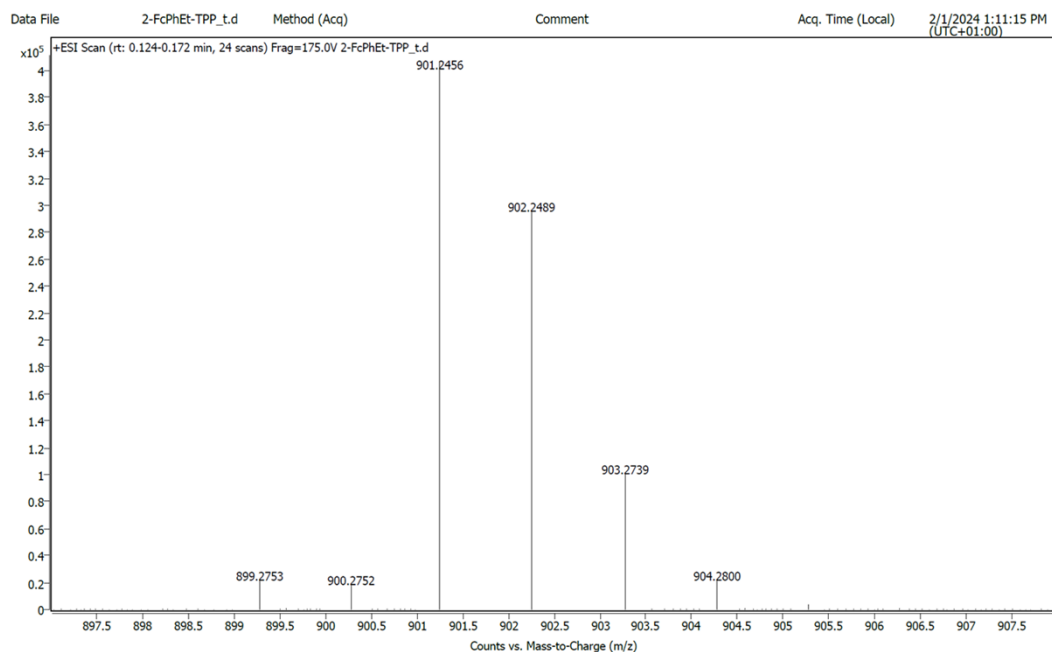
*Fig. S 14 HR-ESI MS of **6t**, (E) 2-(4'-ferrocenylstyryl)-5,10,15,20-tetraphenylporphyrin (trans-isomer).*

Characterisation data for compound 6α (α) 2-(4'-Ferrocenylstyryl)-5,10,15,20-tetraphenylporphyrin (*alpha*-isomer)
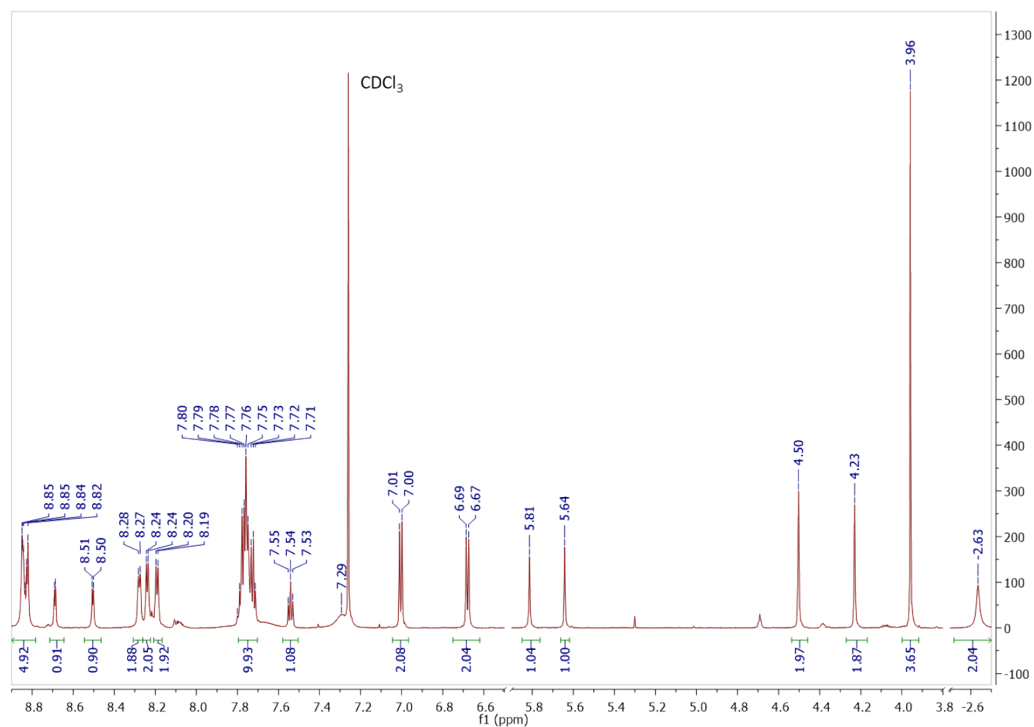
Fig. S 15 ^{1}H-NMR (700 MHz, CDCl$_3$) of compound **6α**, (α) 2-(4'-ferrocenylstyryl)-5,10,15,20-tetraphenylporphyrin (alpha-isomer).
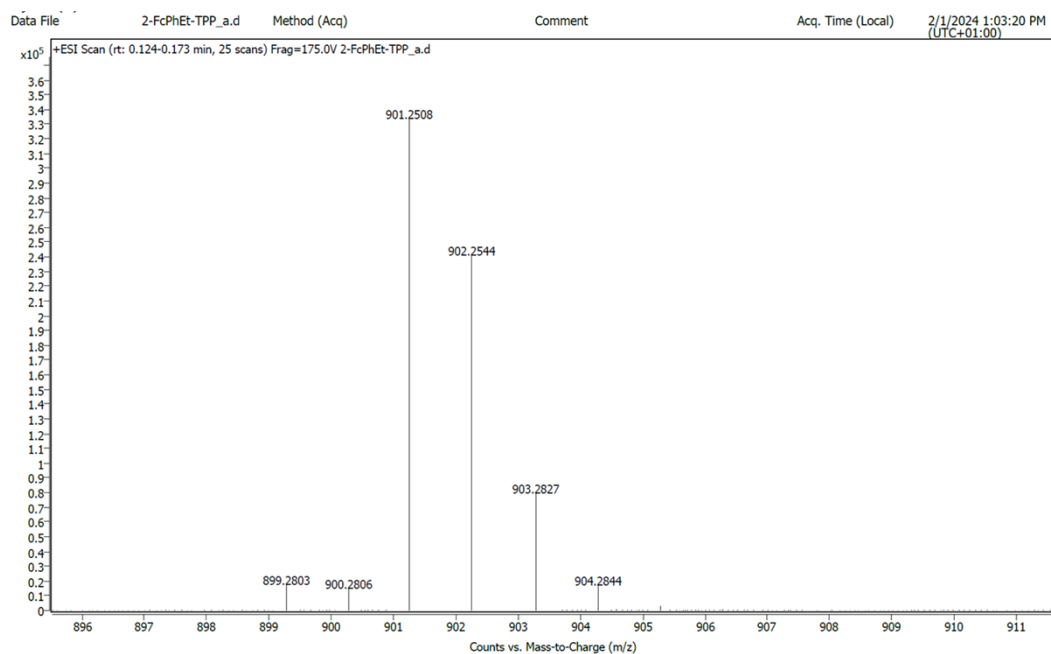
Fig. S 16 HR-ESI MS of **6α**, (α) 2-(4'-ferrocenylstyryl)-5,10,15,20-tetraphenylporphyrin (alpha-isomer).

Characterisation data for compound 7*t* (E) 2-styryl-5,10,15,20-tetraphenylporphyrin (*trans*-isomer)
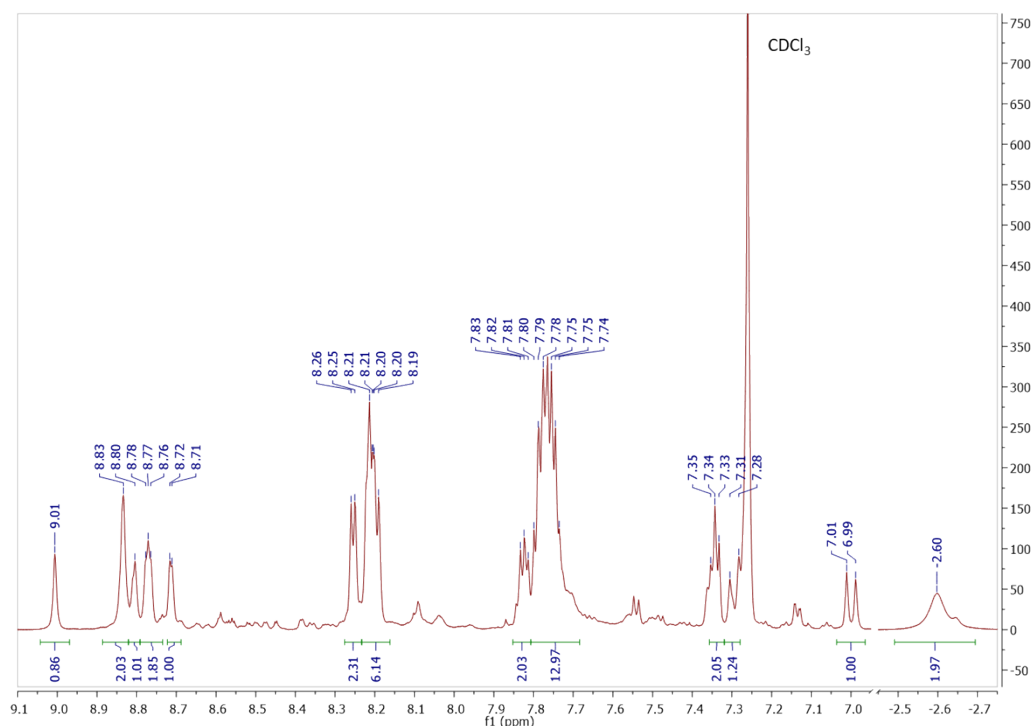
*Fig. S 17 ^{1}H-NMR (700 MHz, CDCl$_3$) of compound **7t**, (E) 2-styryl-5,10,15,20-tetraphenylporphyrin (trans-isomer).*
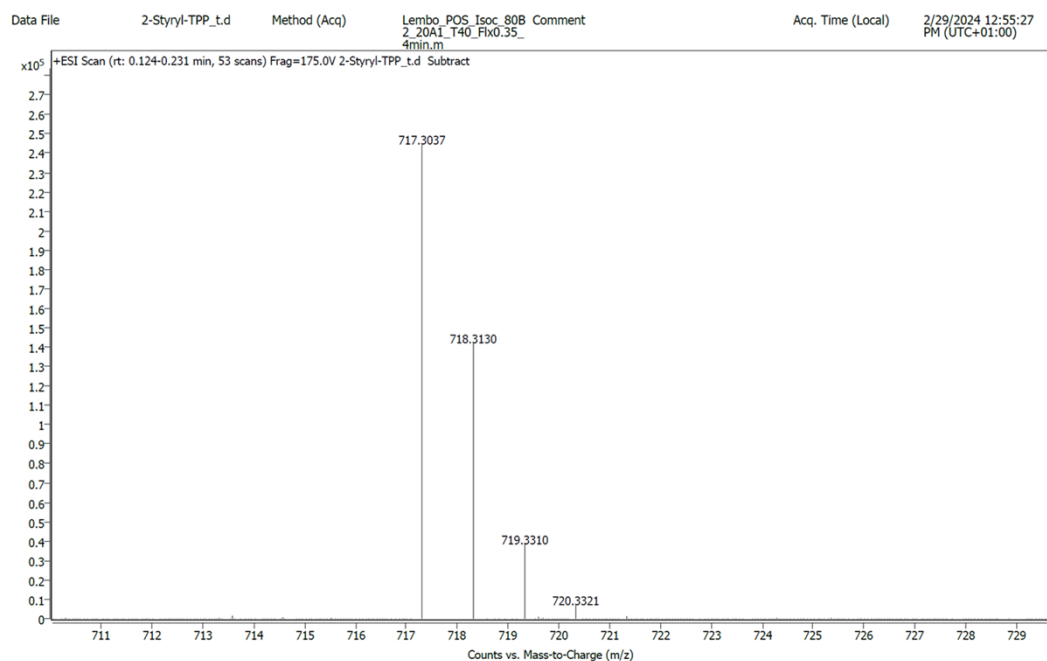
*Fig. S 18 HR-ESI MS of **7t**, (E) 2-styryl-5,10,15,20-tetraphenylporphyrin (trans-isomer).*

Characterisation data for compound 7α (α) 2-styryl-5,10,15,20-tetraphenylporphyrin (*alpha-isomer*)
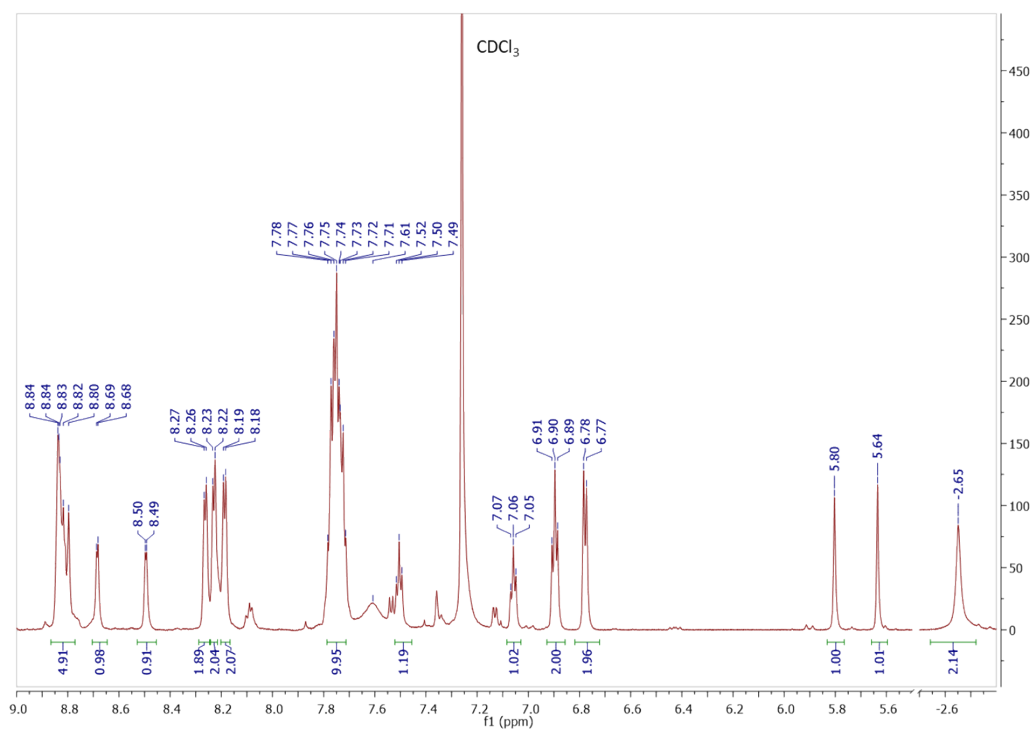
*Fig. S 19 ^{1}H-NMR (700 MHz, CDCl$_3$) of compound **7α**, (α) 2-styryl-5,10,15,20-tetraphenylporphyrin (alpha-isomer).*
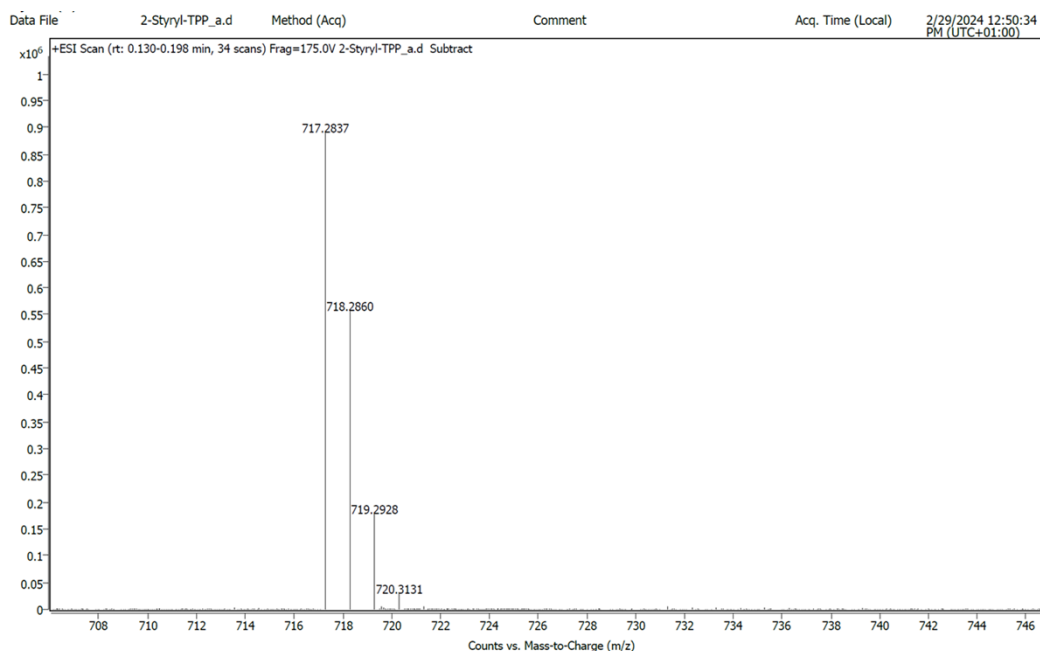
*Fig. S 20 HR-ESI MS of **7α**, (α) 2-styryl-5,10,15,20-tetraphenylporphyrin (alpha-isomer).*

Characterisation data for compound 9*t* (E) 1-Ferrocenyl-2-phenylethene (*trans*-isomer)
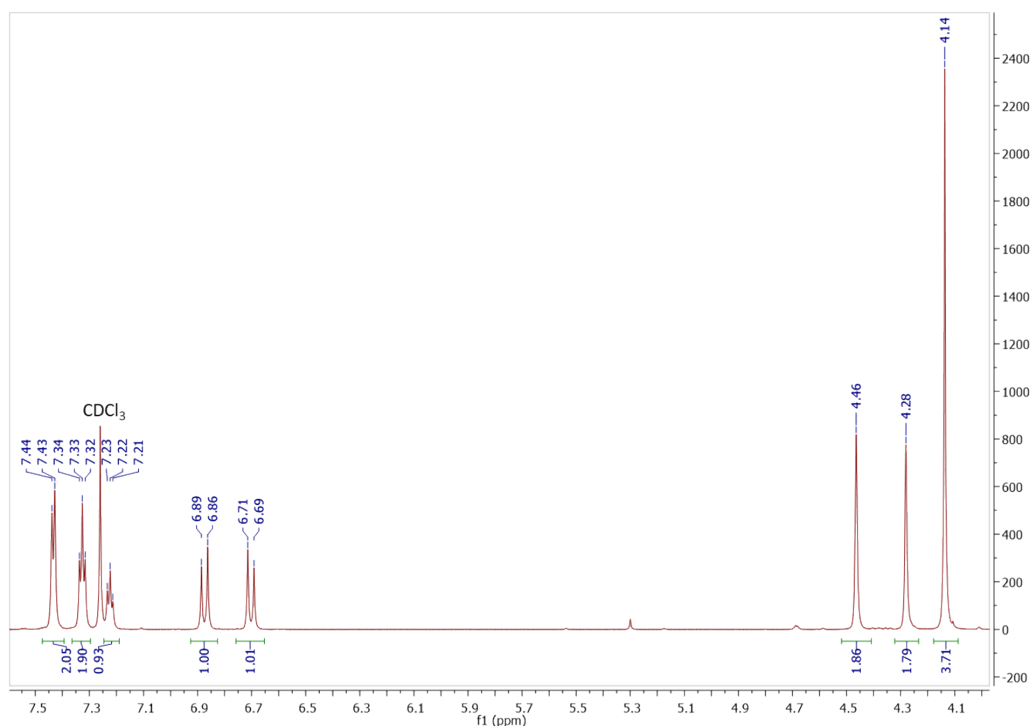
*Fig. S 21 ^{1}H-NMR (700 MHz, CDCl$_3$) of compound **9t**, (E) 1-ferrocenyl-2-phenylethene (trans-isomer).*

Line#:1 R.Time:18.100(Scan#:2821)
MassPeaks:352
RawMode:Averaged 18.095-18.105(2820-2822) BasePeak:288(99688)
BG Mode:Calc. from Peak Group 1 - Event 1 Scan
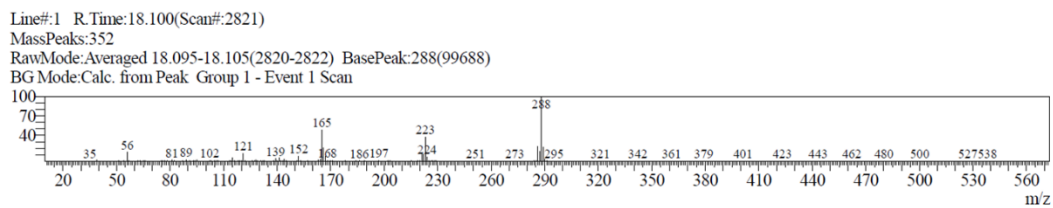
*Fig. S 22 GC-MS characterisation, mass spectrum of compound **9t** ((E) 1-Ferrocenyl-2-phenylethene, trans-isomer), r.t. = 18.1 min.*

Characterisation data for compound 9α (α) 1,1-ferrocenyl-phenylethene (*alpha*-isomer)
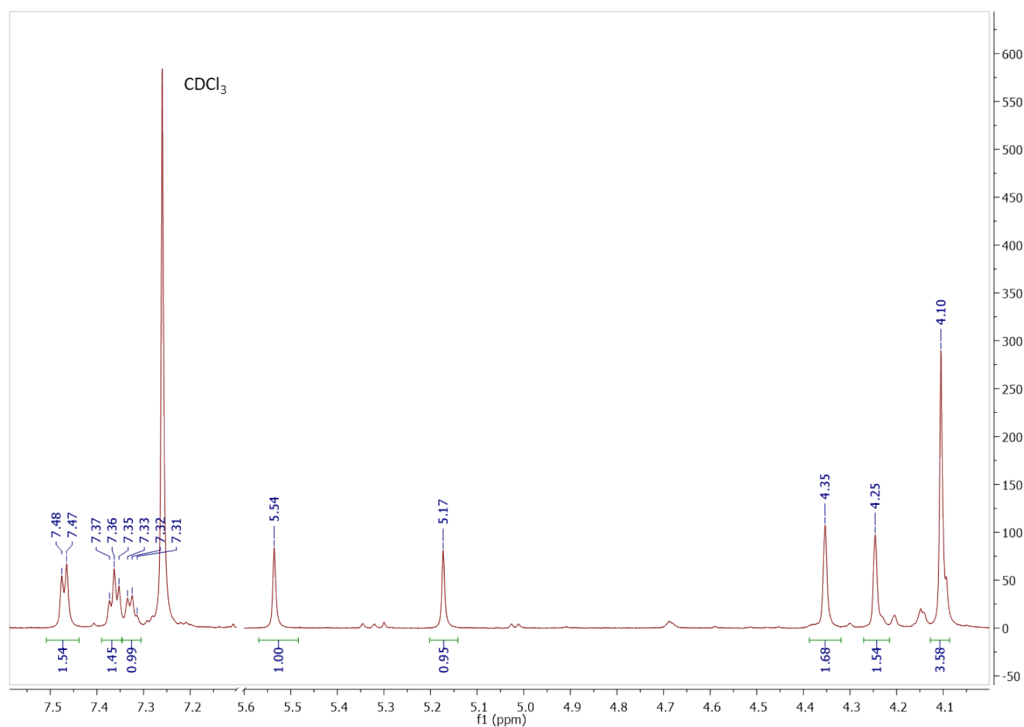
*Fig. S 23 ^{1}H-NMR (700 MHz, CDCl$_3$) of compound **9α**, (α) 1,1-ferrocenyl-phenylethene (alpha-isomer).*
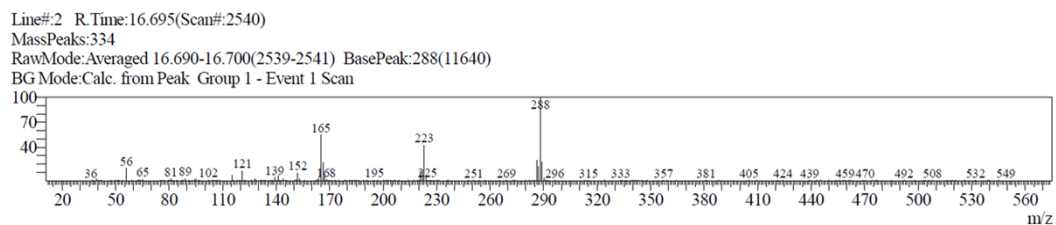
*Fig. S 24 GC-MS characterisation, mass spectrum of compound **9α** ((α) 1-Ferrocenyl-2-phenylethene, alpha-isomer), r.t. = 16.69 min.*

S2.12. Characterisation data for compound 10*t* (E) 4-ferrocenylstilbene (*trans*-isomer)
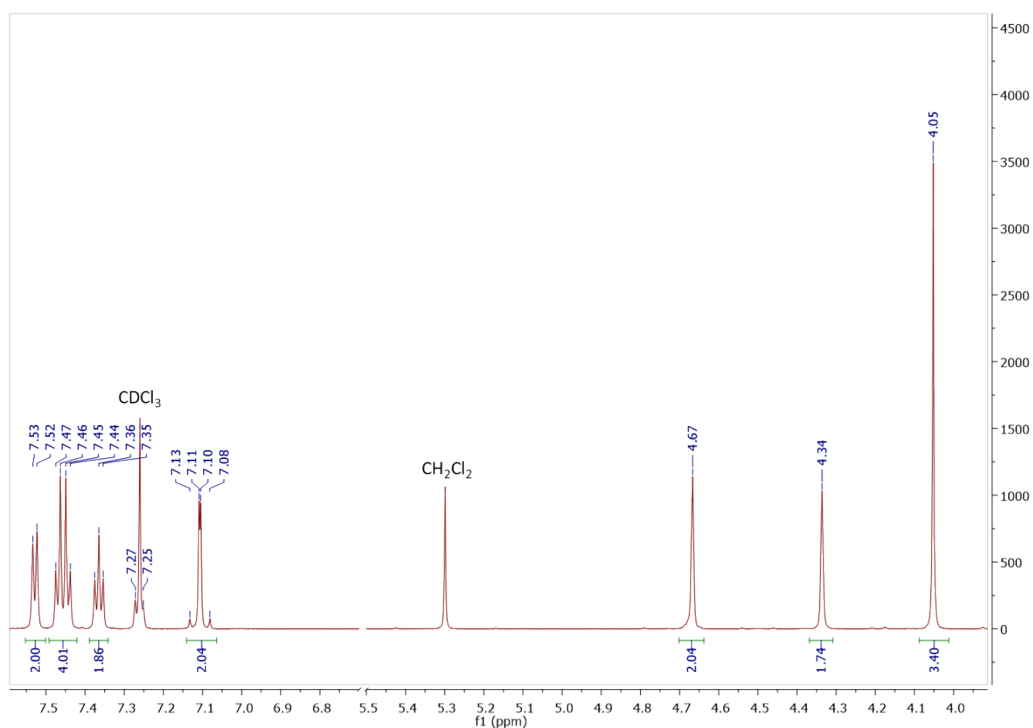
*Fig. S 25 ^{1}H-NMR (700 MHz, CDCl$_3$) of compound **10t**, (E) 4-ferrocenylstilbene (trans-isomer).*
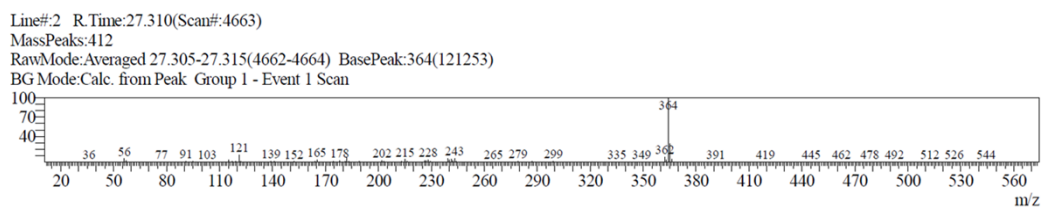
*Fig. S 26 GC-MS characterisation, mass spectrum of compound **10t** ((E) 4-ferrocenylstylebene, trans-isomer), r.t. = 27.31 min.*

S2.13. Characterisation data for compound 10α (α) 4-ferrocenylstilbene (*alpha*-isomer)
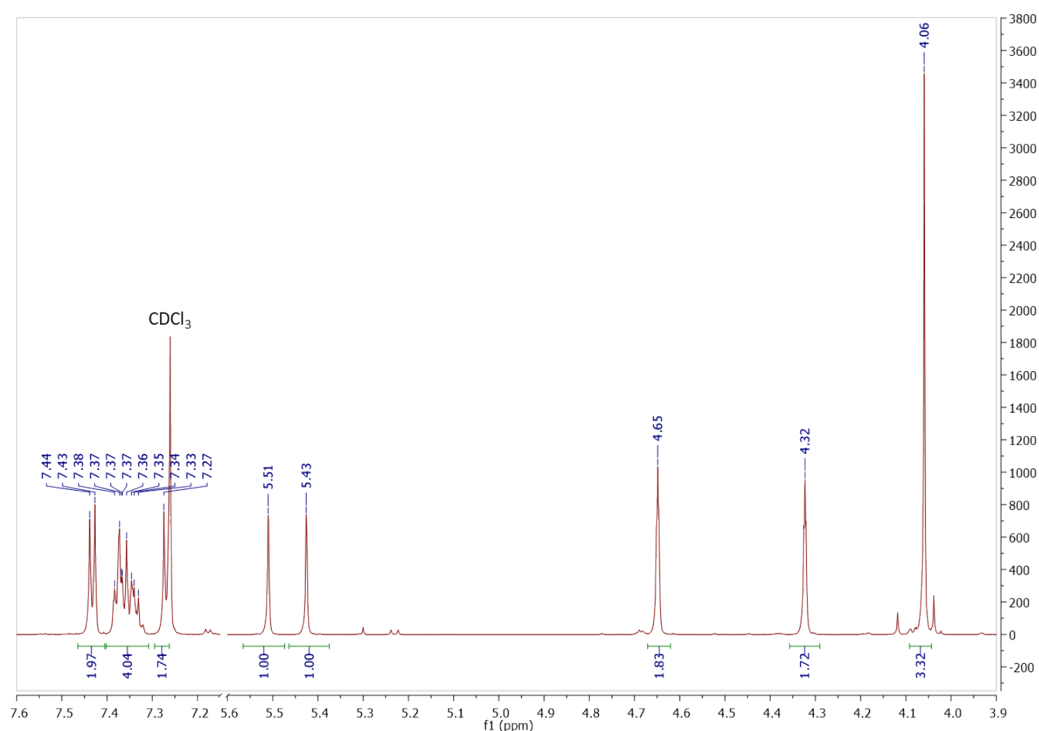
*Fig. S 27 ^{1}H-NMR (700 MHz, CDCl$_3$) of compound **10α**, (α) 4-ferrocenylstilbene (alpha-isomer).*
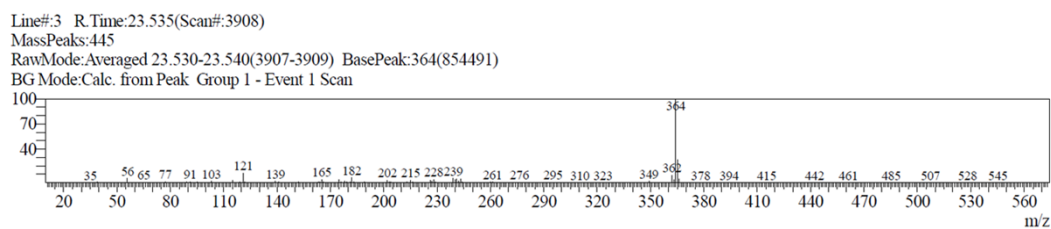
*Fig. S 28 GC-MS characterisation, mass spectrum of compound **10α** ((α) 4-ferrocenylstylebene, alpha-isomer), r.t. = 23.54 min.*

S2.14.   Characterisation data. ¹H-NMR spectra comparison of *meta*- and *para*-phenyl protons of the two isomer 5*t* (*trans*) and 5α (*alpha*)
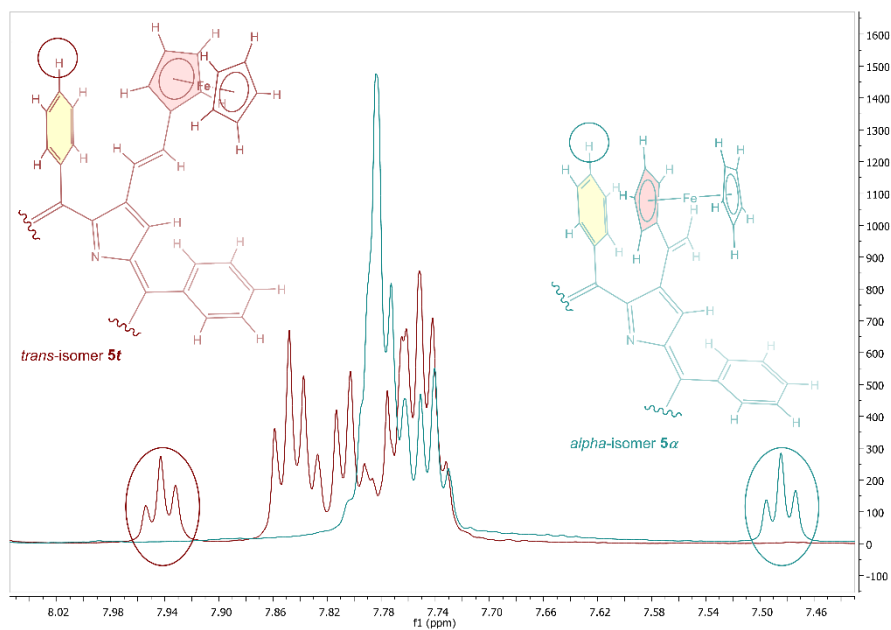
*Fig. S 29 Comparison of ¹H-NMR spectra, recorded in CDCl₃ solution at 298 K, of the two isomers trans-**5t** (dark red) and alpha-**5α** (cyano), showing the downshift of the triplet signal of the proton in relative para-position on the porphyrin meso-phenyl ring attached to C20. This downshift is likely due to strong π-interaction, occurring in the alpha-isomer, between substituted cyclopentadienyl ring of ferrocene (red filled) and the meso-phenyl ring on C20 of the porphyrin ring (yellow filled).*

S2.15.   Characterisation data for the two isomers **5*t*** and **5α**. Bidimensional NMR study

Figure S30 shows the ^{1}H-NMR spectrum of one of the products **5α** obtained from the Heck coupling between β-brominated porphyrin and vinylferrocene. Analysis of the signals revealed the presence of the expected seven pyrrolic hydrogens between 8.6 and 9.0 ppm. However, the region between 7.5 and 8.4 ppm showed signals of only three phenol rings plus a triplet that integrates for one proton. Two signals in the region between 5.1 and 5.5 ppm were tentatively assigned to protons attached to sp2 carbons. Finally, a signal integrating for five hydrogens at 4.0 ppm was assigned to the unsubstituted ring of ferrocene, whereas the two expected signals of the substituted ring were not observed.
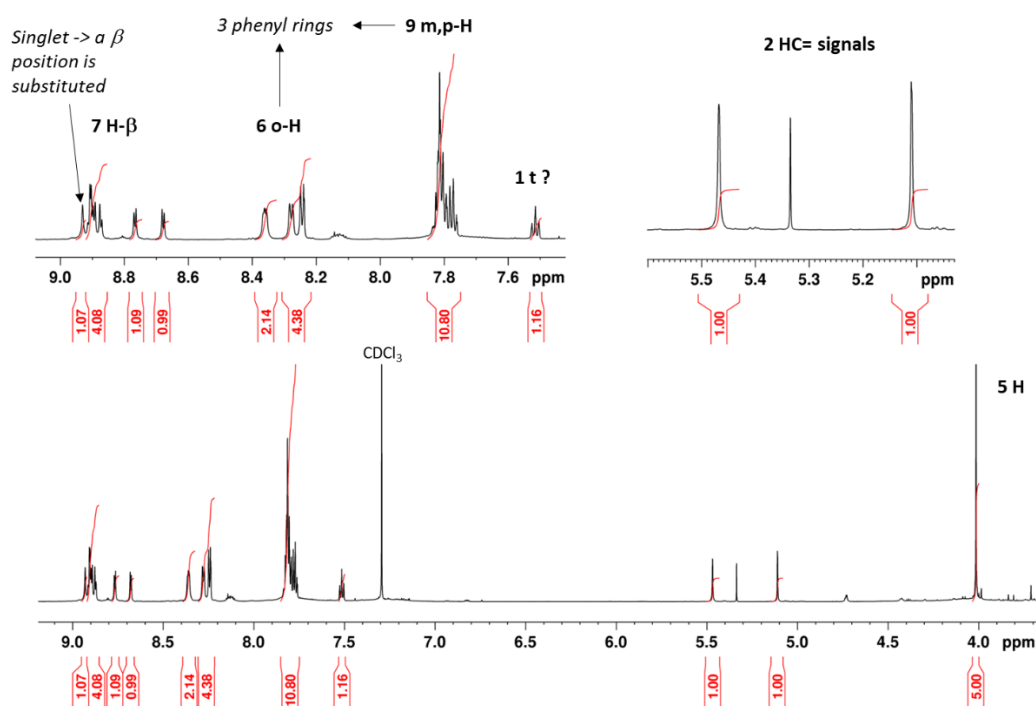
Fig. S 30 ^{1}H-NMR at 700 MHz (298 K) of a product from the Heck coupling between β-brominated porphyrin and vinylferrocene dissolved in CDCl₃. In red are the relative integrals.

The zoom of the [1]H-^{13}C multiplicity edited HSQC shown in Figure S31 A confirmed the assignment of the signals belonging to the observable phenyl rings. Figure S31 B shows that the observed carbon chemical shift is compatible with the ferrocene assignment. Signals corresponding to the six β-pyrrolic are very broad, probably due to an exchange process. The triplet at 7.6 ppm shows a correlation with a phenyl carbon; this fact, in addition to its integral value and multiplicity, allowed us to assign this signal to the para position of the fourth phenyl ring (Figure S31 A). Figure S31C shows the correlation of the two signals at 5.3 and 5.5 ppm with an oppositive phase with respect to the other signals. This reveals that they belong to a CH_2 group. Given their chemical shift, we can assign them to a terminal position of a double bond.

Raising the temperature to 318 K yielded the appearance of broad signals bolded in yellow in Figure S32 A.
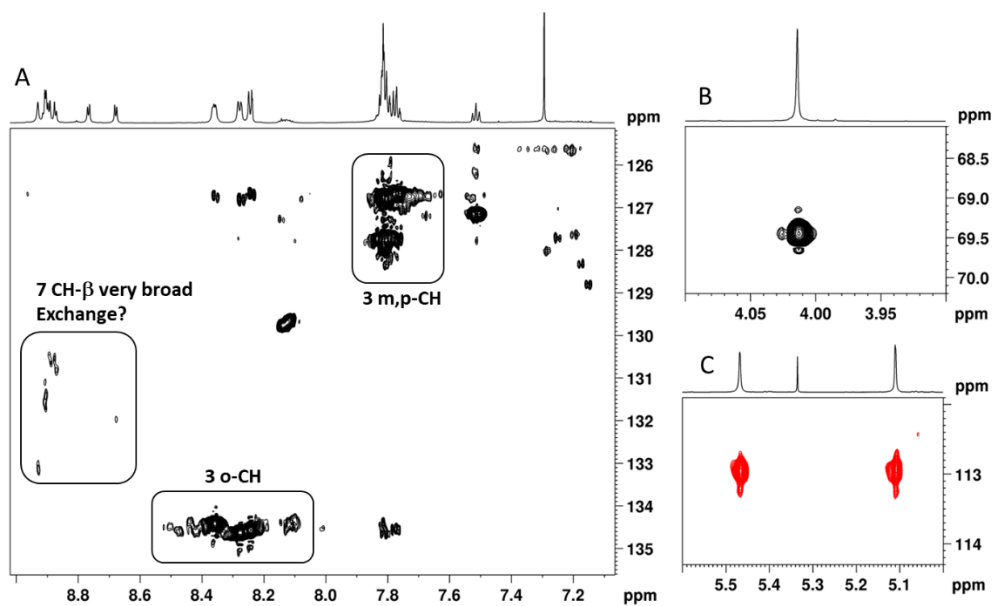
Fig. S 31 ^{1}H-^{13}C multiplicity edited HSQC of three different regions. Positive (black) and negative (red) signals are relative to CH and CH$_2$ groups, respectively.
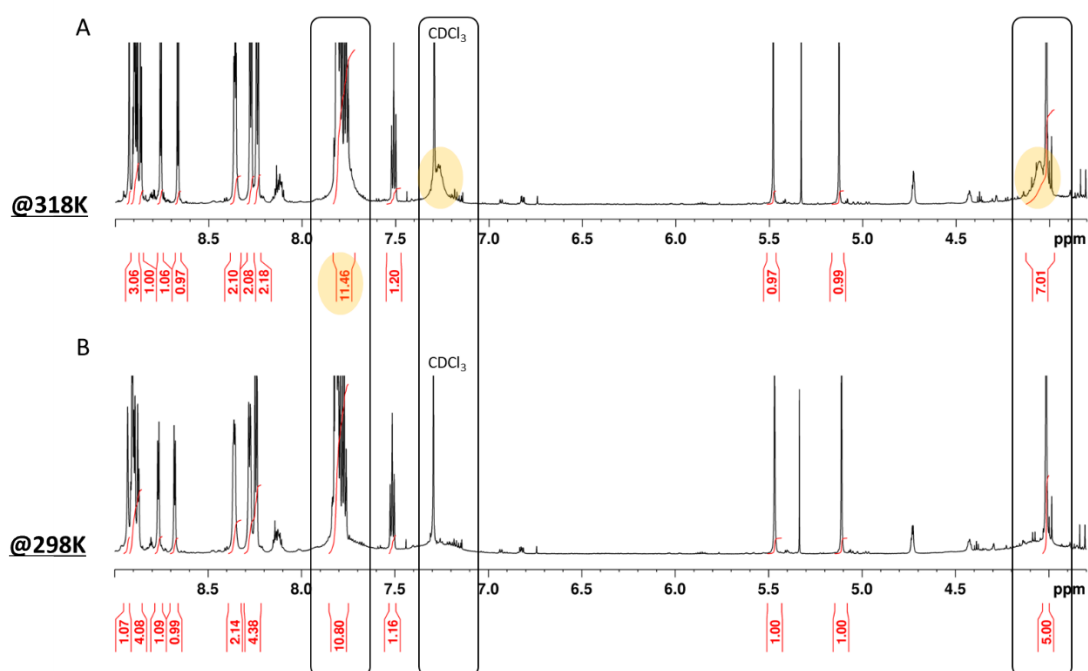
Fig. S 32 Comparison of the ^{1}H-NMR spectra of the same compound recorded at 318 K (A) and 298 K (B).

The ^{1}H-^{1}H COSY experiment unveiled the coupling between the triplet at 7.5 ppm and the broad signal at 7.3 ppm, indicating that this signal corresponds to the meta-proton of the fourth phenyl ring (Figure S33).
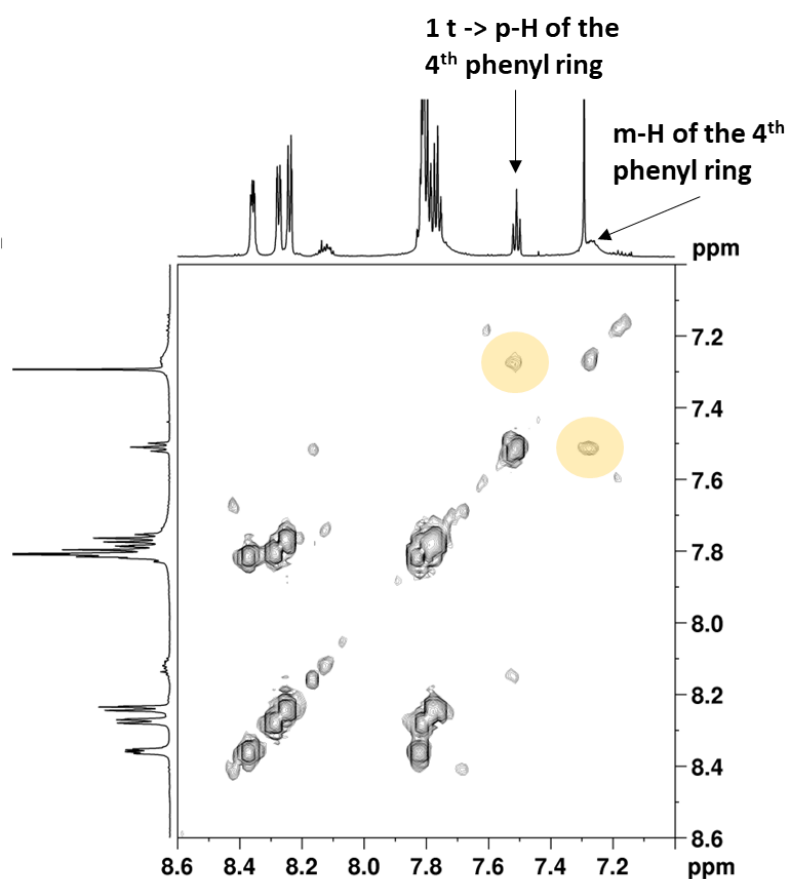
Fig. S 33 A Region of the ^{1}H-^{1}H COSY at 318 K confirms the meta-proton assignment of the fourth phenyl ring.

Figure S34 compares two regions of the ^{1}H-^{13}C HSQC recorded at two different temperatures. At the higher temperature (Figure S34 B), we observed the correlation of the three broad signals detected in the proton spectrum of Figure S32 A. In addition to the already assigned signal at 7.3 ppm belonging to the *meta*-CH groups of the fourth phenyl ring, we could assign the signal at 7.8 ppm as the *ortho*-CHs of the same ring and the broad signal 4.05 ppm to two CHs of the substituted ferrocenyl ring (Figure S34 B).

All these results converge to the possible structure in Figure S35. Due to the proximity of the phenyl ring and the ferrocene, there is a hindered rotation of these groups, which leads to the broadening of the ortho- and meta-signals of the phenyl group. Similarly, the CH group of the unsubstituted ring of the ferrocene also experiences broadening due to an intermediate exchange regime. This occurs because the phenyl ring and the ferrocene are so close together that they cannot rotate freely, affecting these groups' signals. The para-hydrogen signal is sharp even at 298 K due to conformational shift and rotation around the phenyl axis, which does not affect its chemical shift.
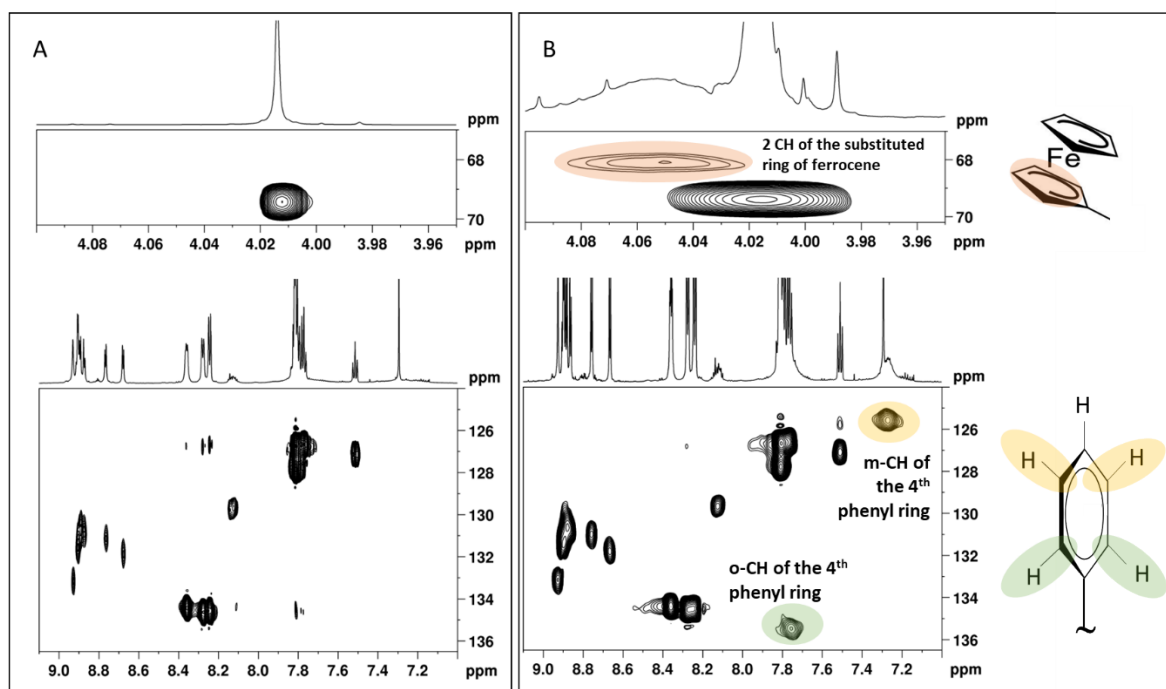
Fig. S 34 Comparison of two regions of ^1H-^{13}C HSQC recorded at two different temperatures: 298 K (A) and 318 K (B).

The ^1H-^1H ROESY and ^1H-^{13}C HMBC experiments confirmed this structure as the *alpha*-isomer. Figure S36 shows the diagnostic short distances from the ROESY experiment and the long-range proton-carbon couplings from the HMBC.
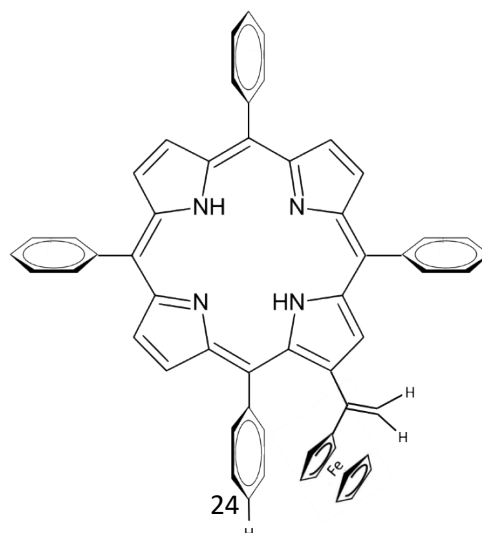
Fig. S 35 Proposed structure for one of the unknown products from the Heck coupling between β-brominated porphyrin and vinylferrocene dissolved in CDCl₃.
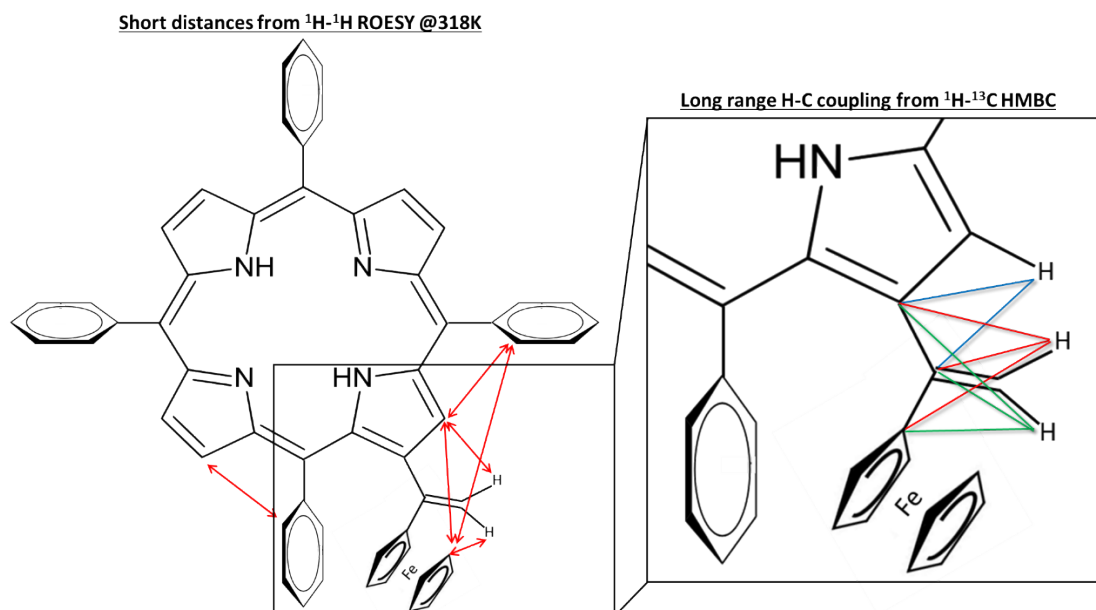
Fig. S 36 Arrows indicate the distances observed with ROESY and HMBC diagnostic of the structure of the alpha-isomer.

The spectrum of the second product of the reaction **5t** is shown in Figure S37. Differently from the previous compound, this spectrum shows all the expected signals. In particular, the region between 7.2 and 6.5 ppm shows the presence of two doublets with a coupling constant of 16 Hz, indicating that they are positioned in *trans*. In addition to this information, a complete set of bidimensional NMR experiments was recorded, allowing us to confirm the structure of the H$_2$-2-(ferrocenyl)vinyl-5,10,15,20-tetraphenylporphyrin *trans*-isomer.
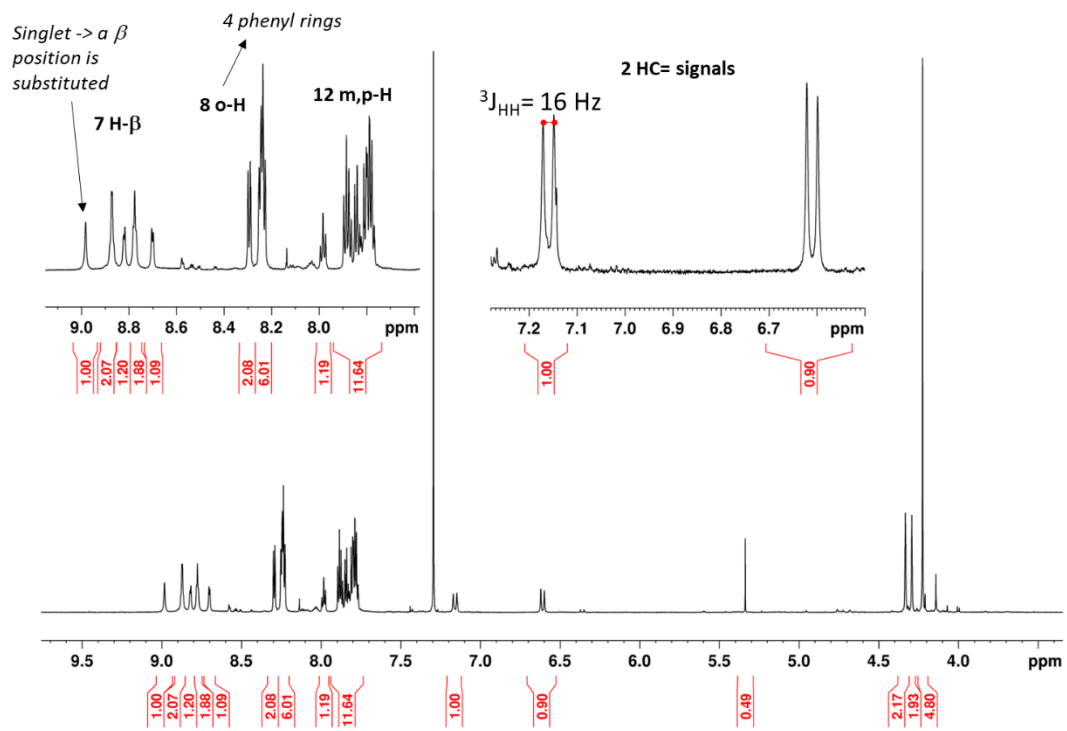
Fig. S 37 ¹H-NMR spectrum of H₂-2-(ferrocenyl)vinyl-5,10,15,20-tetraphenylporphyrin trans-isomer at 700 MHz (298 K) in CDCl₃

S3. Cyclic Voltammetry measurements

S3.1.   Cyclic voltammetry of free ferrocene as reference compound
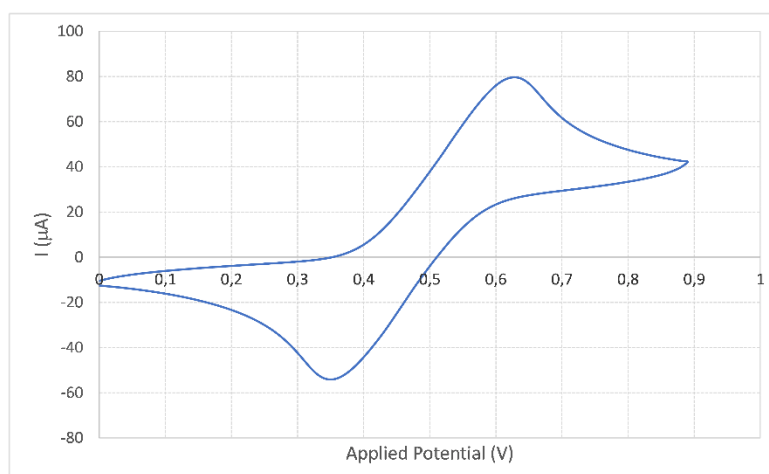
Fig. S 38 Cyclic Voltammetry of 2mM ferrocene in 0.1M TBAP dichloromethane solution recorded at 10 mV step and 100mV/s rate.

S3.2. CV and DPV measurements of the two isomers 5*t* and 5α
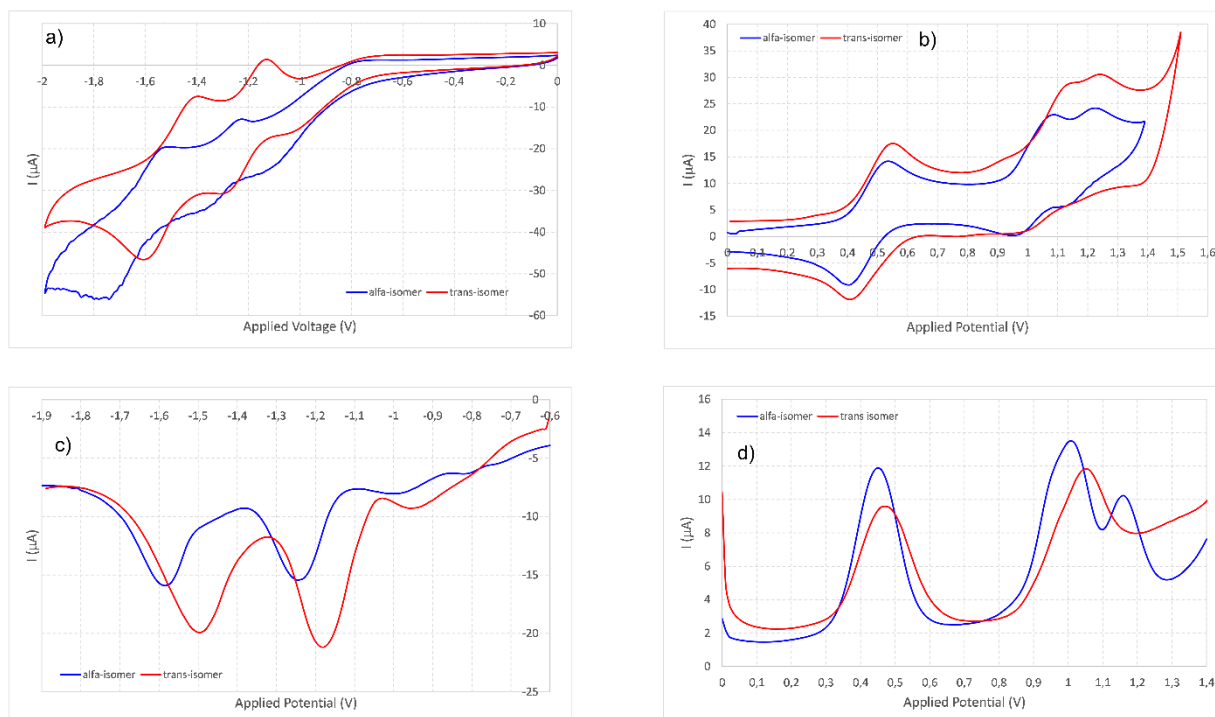
*Fig. S 39 **5t** (0.75 mM, red line) and **5α** (1mM, blu line) electrochemical characterisation in 0.1 M TBAP dichloromethane solution. a) cyclic voltammetry cathodic scan, b) cyclic voltammetry anodic scan; c) differential pulse voltammetry cathodic scan and d) differential pulse voltammetry anodic scan. In DPV cathodic scan it's possible to observe a small shoulder between -0.9 V and -1.1 V in both isomers, most likely due to an irreversible electrochemical reaction involving ethylene bridge. Something similar is also observable in the respective anodic scan, between 0.9 and 1 V but to a minor extent.*

S3.3. CV and DPV measurements of ferrocene reference compounds 9*t*, 9α, 10*t*, 10α
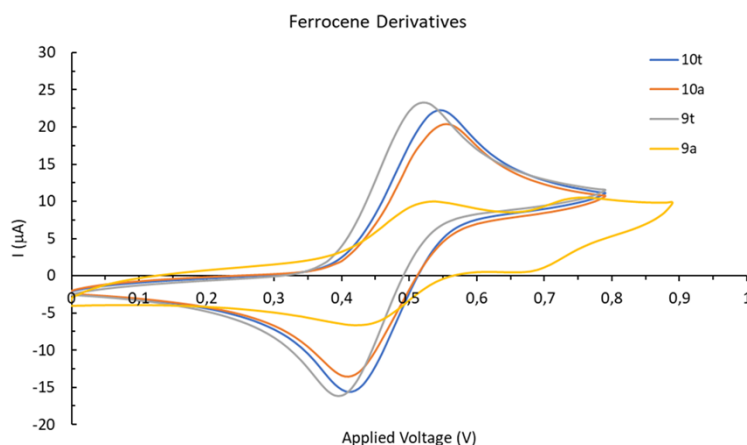
*Fig. S 40 Cyclic Voltammetry of 1mM solution of ferrocene reference compounds **9t** (1-ferrocenyl-2-phenylethene_trans), **9α** (1,1-ferrocenyl-phenylethene_alpha), **10t** (4-ferrocenylstilbene_trans) and **10α** (4-ferrocenylstilbene_alpha) in 0.1M TBAP dichloromethane solution recorded at 10 mV step and 100mV/s rate. The reference compound **9α** is not stable under analytical conditions and the second wave observable at about 0.7 V can be ascribable to chemical reaction occuring on the electrode surface.*

29

S3.4.   CV and DPV measurements of the two isomers 6*t* and 6α
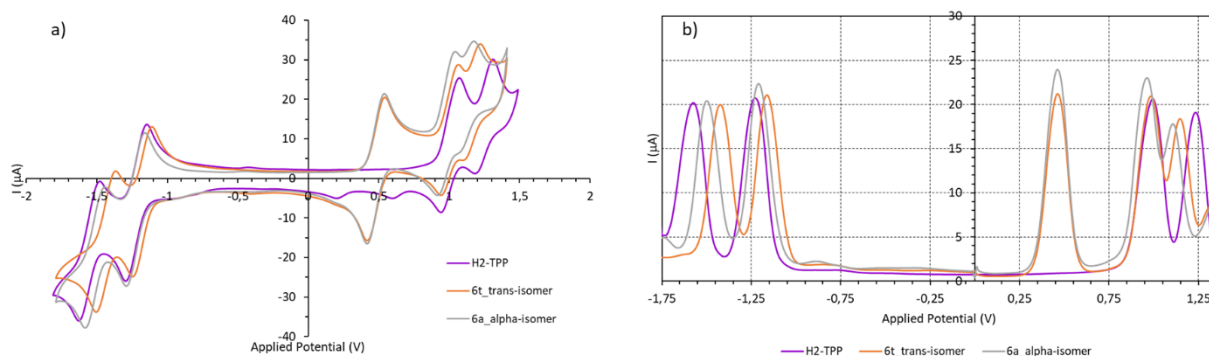
*Fig. S 41 **H₂TPP** (1 mM purple line), **6t** (1mM, orange line) and **6α** (1mM, gray line) electrochemical characterisation in 0.1 M TBAP dichloromethane solution. a) cyclic voltammetry cathodic-anodic scan, b) differential pulse voltammetry cathodic and anodic.*

S4. Photochemical characterisation data

UV-vis absorption spectra of ferrocene reference compounds 9*t*, 9α, 10*t*, 10α
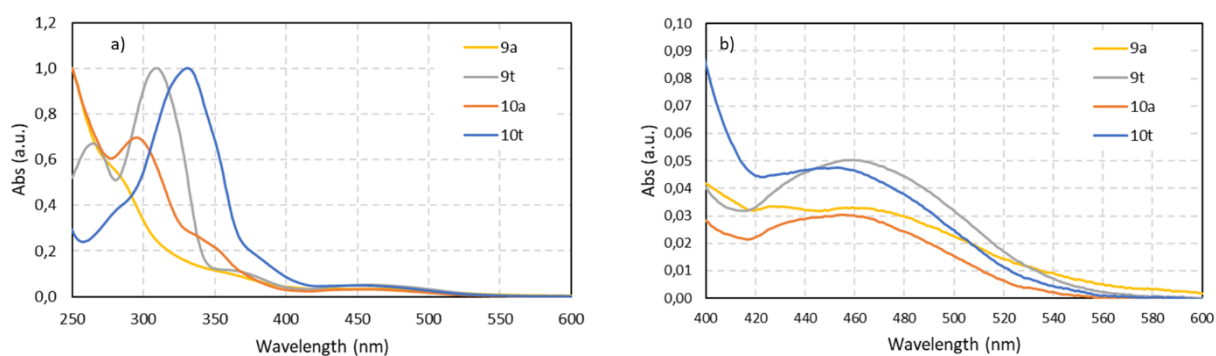
*Fig. S 42 Normalized UV-vis spectra of ferrocene reference compounds **9t, 9α, 10t** and **10α** recorded in dichloromethane solution. a) Whole spectrum. b) Zoom-in in the longer wavelength region.*

Fluorescence Excitation spectra of compounds 5*t*, 5α, 6*t*, 6α, 7*t* and 7α
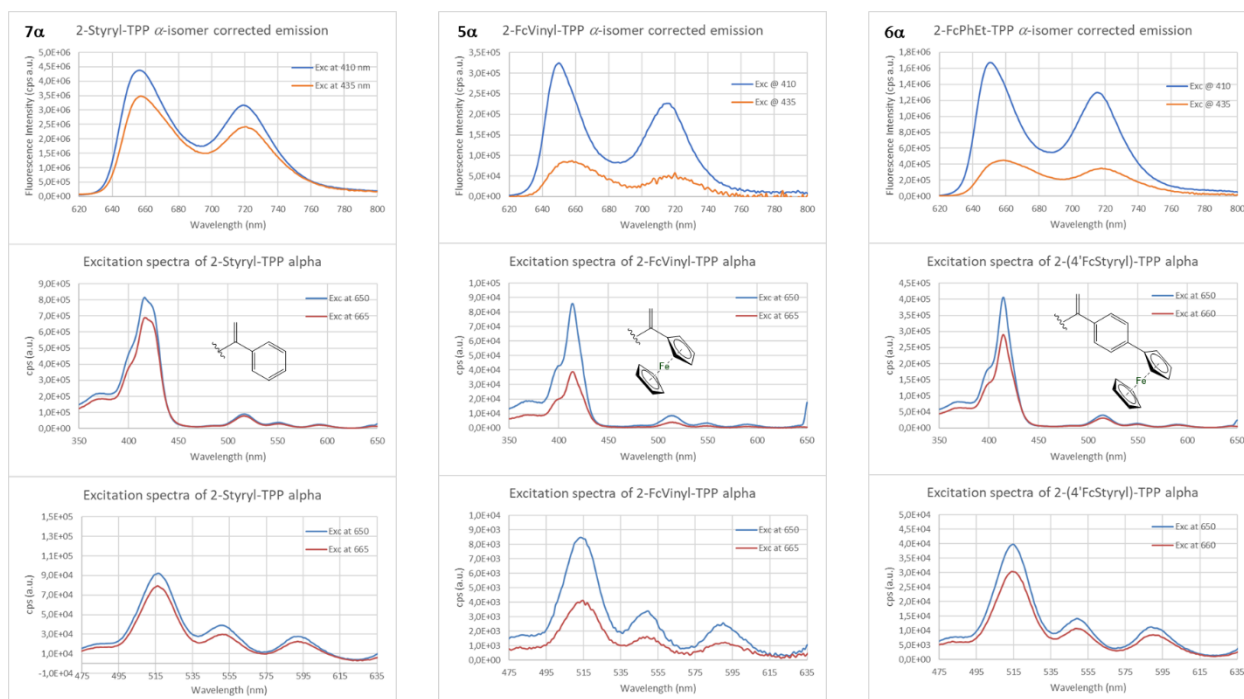
*Fig. S 43 Fluorescence excitation spectra of alpha-isomers of compound **5** (central coloumn) **6** (right coloumn) and **7** (left coloumn). In the first row the emission spectra of each compound was reported, exciting on both the blue (410 nm) and red (435 nm) side of the Soret band. In the second row the corresponding excitation spectra were reported. In the third row a zoom-in on the porphyrin Q bands were reported. Porphyrin beta-substituents are depicted in the central row on their respective excitation spectra. No $\lambda_{exc.}$ dependence emission was observed for the alpha-isomers.*
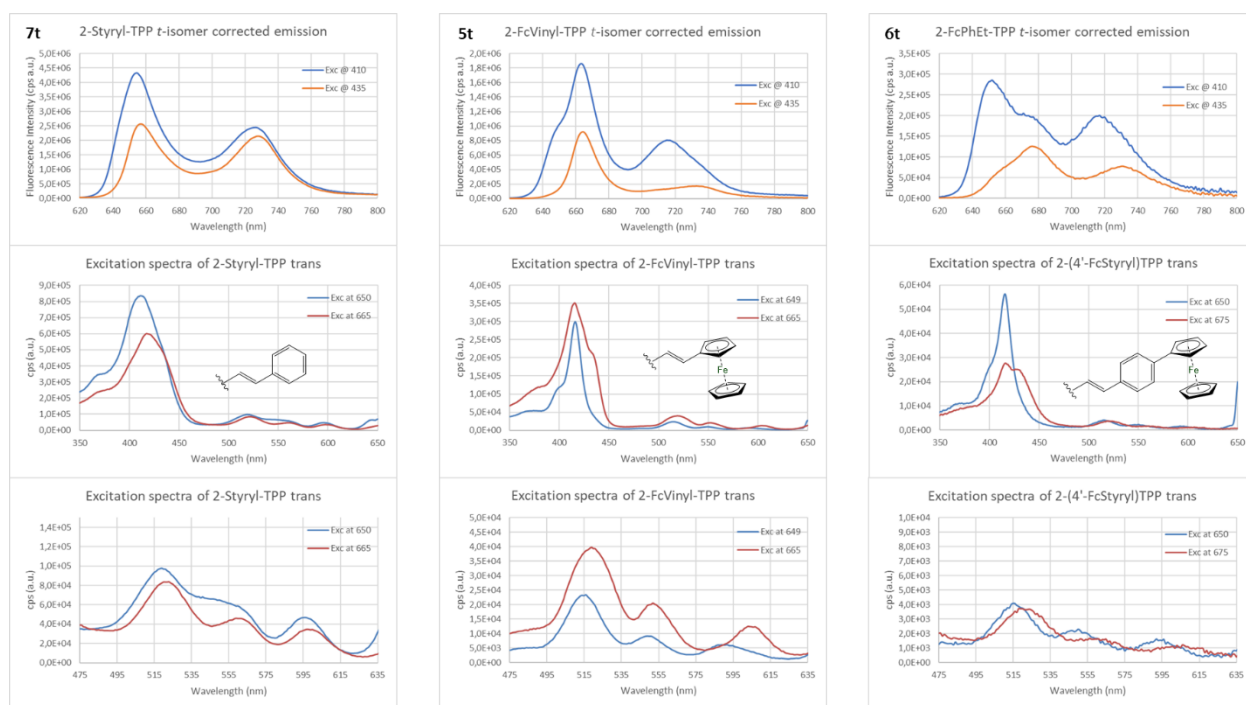
*Fig. S 44 Fluorescence excitation spectra of trans-isomers of compound **5** (central coloumn) **6** (right Coloumn) and **7** (left coloumn). In the first row the emission spectra of each compound was reported, exciting on both the blue (410 nm) and red (435 nm) side of the Soret band. In the second row the corresponding excitation spectra were reported. In the third row a zoom-in on the porphyrin Q bands were reported. Porphyrin beta-substituents are depicted in the central row on their respective excitation spectra. $\lambda_{exc.}$ dependence emission is clearly observable.*

Fluorescence emission of ferrocene and H₂TPP (7.8 μM) 1:1 ratio in dichloromethane solution.
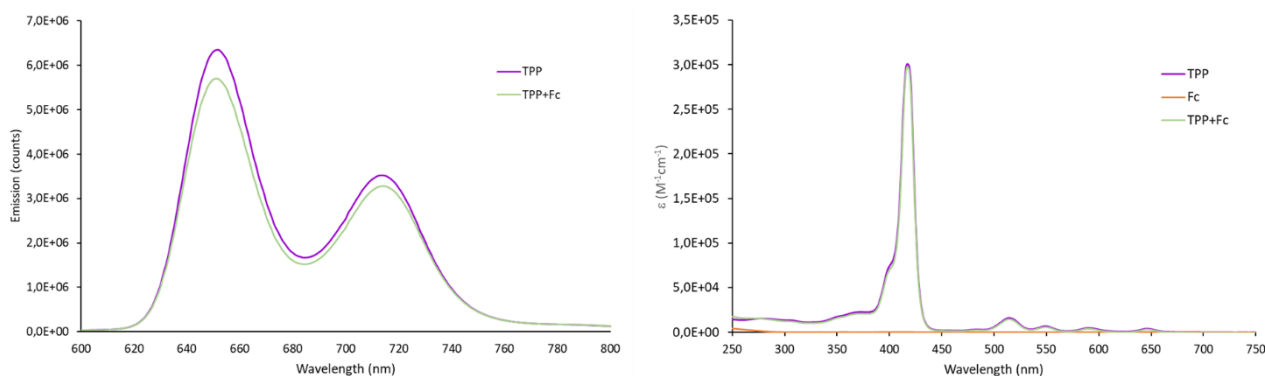
Fig. S 45 Fluorescence emission spectra of H_2TPP and an equimolar amount of H_2TPP and Ferrocene in 1:1 ratio (7.8 μM) in dichloromethane solution (left) along with the corresponding UV-vis aborbance spectrum (right). Porphyrin fluorescence was normalized for the absorbance value (≈0.1) at excitation wavelength (515 nm).

The fluorescence emission spectra of an equimolar concentration (7.8 μM) of H₂TPP and Ferrocene at 1:1 ratio was recorded in dichloromethane solution and compared to that of the only H₂TPP with equal concentration (λ_{exc} = 515 nm). In the H₂TPP/ferrocene mixture, the porphyrin fluorescence was quenched by only 8%, showing a possible electron-transfer under diffusive control occurring on a timescale slower than those observed in the porphyrin-ferrocene

dyads. This aspect can further confirm the important role played by the different linkers in favouring the intramolecular electron-transfer process in all the *alpha-* and *trans*-isomers of the porphyrin-ferrocene dyads.

Time resolved fluorescence measurements of compounds 5t, 5α, 6t, 6α, 7t and 7α
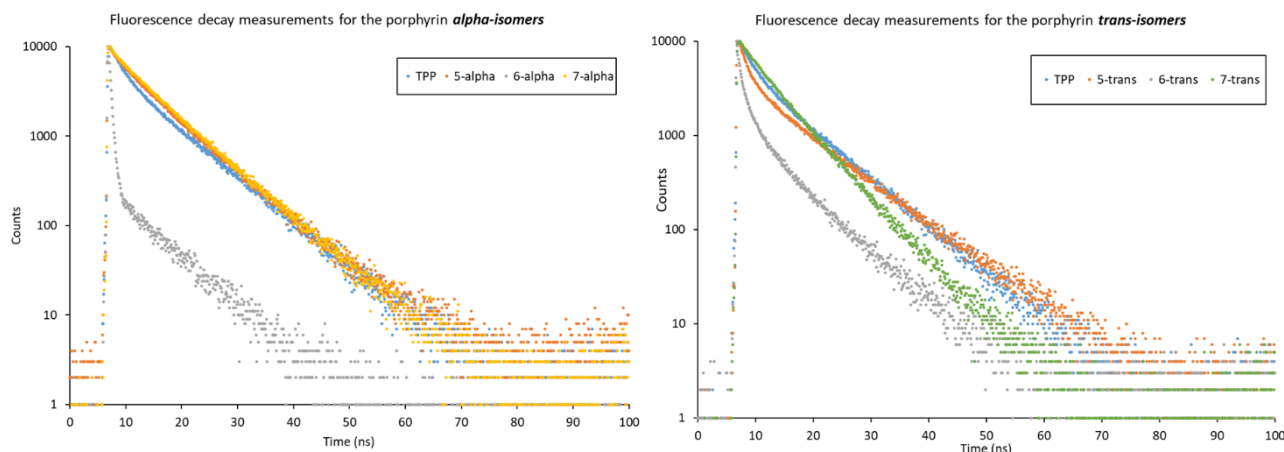
Fig. S 46 Time resolved fluorescence decay of compounds 5α, 6α, and 7α on the left and compounds 5t, 6t and 7t on the right, recorded in dichloromethane solution after laser excitation at 440 nm.

Compound	τ_1 (ns)	τ_2 (ns)	B1	B2	χ^2	ϕ	$\phi/\phi_{7\alpha}$	$<\tau>$	$<\tau>/<\tau>_{7\alpha}$
H$_2$TPP	9.07±0.04	2.23±0.03	4394	4345	1.099	0.11	-	5.67	-
7α	7.66±0.03	1.9±0.1	8362	1612	1.21	0.094	1.000	6.73	1.000
6α	0.415±0.005	7.51±0.09	4814	240	0.979	$9.8\cdot10^{-3}$	0.104	0.75	0.112
5α	7.87±0.04	2.6±0.1	7130	2293	1.171	$1.2\cdot10^{-3}$	0.013	0.98	0.978

Table S 1 Fitting results for H$_2$TPP and alpha-isomers 7α, 6α and 5α. Fluorescence lifetime $\tau_{1/2}$, respective coefficient B1 and B2, χ^2, fluorescence quantum yield ϕ, fluorescence quantum yield ratio $\phi/\phi_{7\alpha}$, average lifetime $<\tau>$ and averaged lifetime ratio $<\tau>/<\tau>_{7\alpha}$ are reported.

Compound	τ_1 (ns)	τ_2 (ns)	B1	B2	χ^2	ϕ	ϕ/ϕ_{7t}	$<\tau>$	$<\tau>/<\tau>_{7t}$
H$_2$TPP	9.07±0.04	2.23±0.03	4394	4345	1.099	0.11	-	5.67	-
7t	6.44±0.08	3.5±0.2	7247	2726	1.04	0.084	1.000	5.62	1.000
6t	6.99±0.05	1.30±0.02	1417	3340	1.43	$8.2\cdot10^{-4}$	0.01	3.00	0.533
5t	9.06±0.04	1.46±0.02	3864	5440	1.03	$4.2\cdot10^{-3}$	0.05	4.62	0.821

Table S 2 Fitting results for H$_2$TPP and alpha-isomers 7t, 6t and 5t. Fluorescence lifetime $\tau_{1/2}$, respective coefficient B1 and B2, χ^2, fluorescence quantum yield ϕ, fluorescence quantum yield ratio $\phi/\phi_{7\alpha}$, average lifetime $<\tau>$ and averaged lifetime ratio $<\tau>/<\tau>_{7\alpha}$ are reported.

Time resolved fluorescence experiments carried-out in dichloromethane solution give back the results reported in Table S1 and S2, for *alpha-* and *trans*-isomers respectively. Compound **7α** and **7t** were considered as reference for the *alpha-* and *trans*-isomers of the porphyrin-ferrocene dyads respectively. By comparing the averaged lifetime ratio $<\tau>/<\tau>_{7\alpha}$ of compounds 6α and 5α with respective fluorescence quantum yield ratio $\phi/\phi_{7\alpha}$, it is possible to observe quite similar values for the dyad 6α ($\phi_{6\alpha}/\phi_{7\alpha}$ = 0.10 and $<\tau>_{6\alpha}/<\tau>_{7\alpha}$=0.11), on the contrary this does

not occur for dyad 5α, a similar result was also observed for the *trans*-isomers **5t** and **6t**, whose <τ>/<τ>$_{7t}$ values are much higher than respective φ/φ$_{7t}$ values. This implies that for compounds **5α**, **5t** and **6t** the fluorescence decay due to possible electron-transfer (ET) is too fast to be observed within the instrument timescale (0.1 ns) and we can appreciate and measure the fluorescence lifetime related to possible ET only for the dyad **6α**, whose lifetime value (τ$_1$ = 0.4 ns) is in good agreement with the respective fluorescence quenching compared to compound **7α** used as reference. At the same time these evidences support the hypothesis that the fluorescence quenching has a kinetic nature starting from the porphyrin excited state rather than it is due to a ground state interaction between the two chromophores. An aspect also excluded by cyclic-voltammetry and UV-vis measurements, the first one underlines no variation in the first oxidation and reduction potential of the ferrocene and porphyrin chromophores respectively in all the dyads and, at the same time, we observe almost identical UV-vis spectrum within the two series 7α, 6α, 5α, and 7t, 67, 5t. Two results that reveal no or very small variations in the ground state energy levels within the *alpha*- and *trans*-isomer series respectively. Similar outcomes can be obtained even if H$_2$TPP is used as reference compound.

To assess the thermodinamic feasibility of charge separation (CS) process, the driving force of electron-transfer (ΔG$_{ET}$) was calculated following the Rehm-Weller[S1] approach by using the equations reported below:

$$1) \quad \Delta G_{ET} = e(E_{OxD} - E_{RedA}) - E_{00}^* + \Delta G_s$$

$$2) \quad \Delta G_s = \frac{e^2}{4\pi\varepsilon_0}\left[\left(\frac{1}{2R_D} + \frac{1}{2R_A}\right)\left(\frac{1}{\varepsilon_{ET}} - \frac{1}{\varepsilon_{ref}}\right) - \frac{1}{R_{DA}\varepsilon_{ET}}\right]$$

$$3) \quad \Delta G_{CR} = -e(E_{OxD} - E_{RedA}) - \Delta G_s$$

where E$_{OxD}$ and E$_{RedA}$ are the oxidation and reduction potential of Donor and Acceptor respectively measured by cyclic voltammetry experiments, E*$_{00}$ is the energy of the first excited state of the porphyrin which can be estimated from the intercrossing point of the normalized absorption and emission spectra. The parameters R$_{DA}$, R$_D$, and R$_{DA}$ are calculated from the ground state geometry of the dyad optimized by DFT at the B3LYP/6-31+G(d) level of theory. The R$_D$ and R$_A$ illustrate the radius of the ferrocene donor and porphyrin acceptor, respectively while R$_{DA}$ is the center-to-edge distance between the two chromophores calculated from the ferrocene iron atom to the *β*-substituted carbon atom of the porphyrin. The ε$_{ref}$ and ε$_{ET}$ are the dielectric constant of the reference solvent used in the electrochemical measurement and the solvent used for the determination of the CS. Here, both the electrochemical and fluorescence measurements were performed in dichloromethane (DCM, ε = 8.9), so that the ΔG$_s$ formula can be simplified as follow:

$$\Delta G_s = -\frac{e^2}{4\pi\varepsilon_0\varepsilon_{ET}R_{DA}}$$

Results are reported in the Table S3. The driving force for the charge separation is negative for all the porphyrin-ferrocene dyads and tends to decrease a little with increasing R_{DA} value, neverteless this trend was not observed in the porphyrin fluorescence quenching of the dyads, where compound **6t**, with the highest R_{DA} value, presents also the highest quenching of the porphyrin emission, underlining a possible role of the linker in the process as postulated also for the other compounds **5α**, **5t** and **6α**.

Compound	E^*_{00} (eV)	R_{DA} (Å)	E_{OxD} (Fc)	E_{RedA} (P)	ΔG_{ET} (eV)	ΔG_{CR} (eV)	ΔG_S (eV)
H$_2$TPP	1.91	-	-	-	-	-	-
7α	1.90	-	-	-	-	-	-
7t	1.89	-	-	-	-	-	-
5α	1.91	4.03	0.47	-1.24°	-0.60	-1.31	-0.40
5t	1.87	5.40	0.48	-1.22	-0.47	-1.40	-0.30
6α	1.91	8.25	0.48	-1.23	-0.40	-1.51	-0.19
6t	1.87	9.52	0.48	-1.18	-0.38	-1.50	-0.17

Table S 3 Calculated free energy values of charge recombination (CR), electron-transfer (ET) and solvent reorganization energy (S) following adopting the Rehm-Weller equation 1), 2) and 3). ° = first porphyrin reduction potential from DPV measurements.

Fluorescence emission spectra of dyad 6α in different solvents (toluene, dichloromethane and acetonitrile)
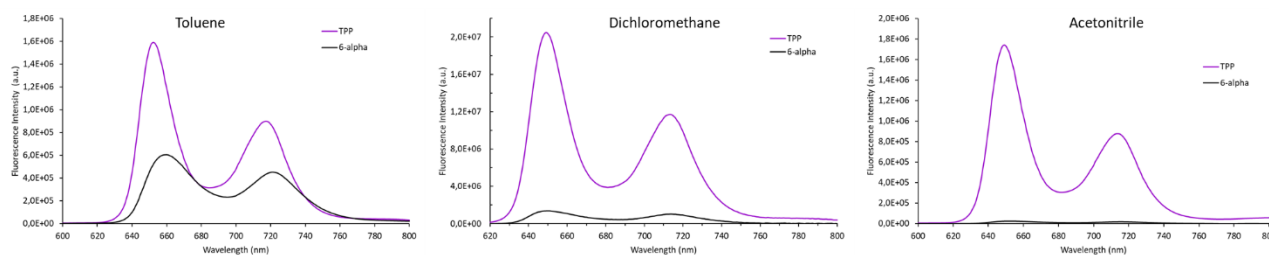
*Fig. S 47 steady-state fluorescence emission of dyad **6α** (black) in different solvents (Toluene-left, dichloromethane-center and acetonitrile-right) compared to that of the H$_2$TPP (purple).*

Dyad **6α** was used as probe to test the solvent effect on the possible electron-transfer mechanism occurring in polar solvents. As it possible to see from the graphs in figure S47 the fluorescence emission of **6α** tends to decrease passing from less polar (toluene ε = 2.4) to much polar solvents (dichloromethane and acetonitrile with ε = 8.9 and ε = 37.5, respectively). The respective fluorescence quantum yields are reported in table S4. The solvent dependent fluorescence quantum yield observed for the dyad **6α** is in line with a possible electron-transfer process as deactivation path of the porphyrin excited state in dichloromethane solution, in accordance with the negative values of the ΔG_{ET} calculated. This observation can be easily transferred to all other dyads that show higher quenching of porphyrin emission in dichloromethane solution.

Compound	φ_toluene	φ_dichloromethane	φ_acetonitrile
H$_2$TPP	0.11	0.11	0.12
6α	0.06	$9.8 \cdot 10^{-3}$	$2.4 \cdot 10^{-3}$

*Table S 4 Porphyrin fluorescence quantum yield for H$_2$TPP[S2] and dyad **6α** in different solvents.*

S5. Computational Study

S5.1.   Energy and maximum absorption wavelength of *trans*- and *alpha*-isomers

The best agreement with experimental UV-VIS data, that was taken as benchmark to assesss the validity of the DFT approach, was found for B3LYP functional and 6-31 G(d) basis set with PCM treatment of the solvent, that predicts the absorption peak maximum with larger accuracy than the other methods tested, in spite of the smaller complexity of the approach. Apparently anomalous trends like this have already been described with PCM calculations of spectroscopic properties in the past, the reason for error cancellations being not always straightforward to be identified. [*L. Gontrani, B. Mennucci, J. Tomasi, "Glycine and alanine: a theoretical study of solvent effects upon energetics and molecular response properties", J. Mol. Struct. Theochem 500 (1-3), 117-127 (2000) 10.1016/S0166-1280(00)00390-0*]. The calculated values for trans and alpha isomers, i. e. the four structures considered in this work that share the same connectivity (stereoisomers), are reported in table S1 and are +3.6 nm and +13.2 nm redshifted with respect to measured spectra in the case of the **5t** and **5α** isomer respectively; the calculated shift between the two isomers is 5.6 nm, slightly higher than the experimental value (4 nm) but overall satisfactory. Similar observation can be done for the ferrocene-porphyrin dyads **6t** and **6α**. It is interesting to notice that in both cases the predicted absorption spectra of the trans-isomers show higher Q/Soret band ratio as reported in the experimental UV-vis spectra. The good reproduction of UV-Vis spectra of the trans-alpha pairs of isomers, made us confident about the validity of the method chosen, and of the (relative) calculated energies as well as of the geometrical parameters of the two isomers. Among the two stereoisomers, the trans form is calculated to have the lower energy, with the alpha form being higher in energy by about 7.3 kCal/mol. The calculated UV-Vis spectrum of the isomers considered in the main article (trans and alpha) are reported in fig S45 as well, with the alpha isomers featuring a main peak at 433.2 nm. The energy of this form is the highest of the pool (+7.28 Kcal/mol), though this energy value should not be directly compared to the trans-isomer, considering that the connectivity is different in this case, owing to the presence of the $CH_2=$ moiety. Regarding the comparison of experimental and calculated optical data, the deviation ranges from 0.9 to 1.8% for the trans-isomers **5t** and **6t** respectively, and about 3% for the alpha form, that is erroneously predicted to have a larger wavelength than the trans form. Interestingly, the computational analysis confirms the larger peak width observed for the trans isomer, that is ascribable to the presence of several contributing vertical transitions of sizeable intensity besides the central one, supporting the view that in this case the conjugation extent is larger. Overall, we can state that the prediction of UV-VIS spectra with the chosen theoretical method is quite satisfactory.

Isomer	Energy (a.u.)	Difference (kCal/mol)	Exp λ_{max}(nm) (DCM)	Theo λ_{max}(nm) (DCM)
5t_Trans	-3640.6745	0	424	427.6
5α_Alpha	-3640.6629	+7.28	420	433.2
6t_Trans	-3640.6745	0	424	431.8
6α_Alpha	-3640.6629	+7.28	421	433.2

Table S 5 Calculated energies and maximum absorption wavelength in the range 200-900 nm
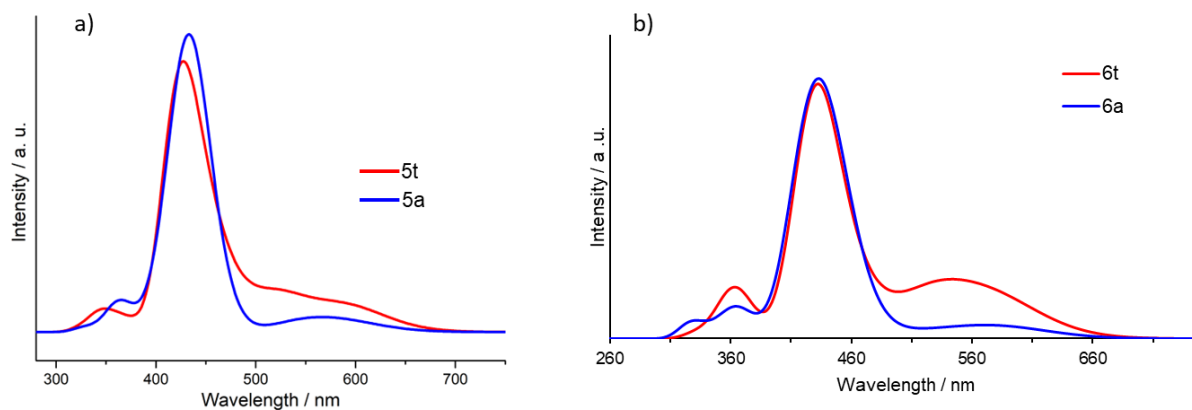
*Fig. S 48 Calculated TD-DFT UV-Vis spectra of trans and alpha isomers of ferrocene-porphyrin dyad **5** and **6** on the left (a) and right (b) part respectively . Trans: red and alpha: blue. Dichloromethane solvent effect is modelled with PCM method.*

Regarding the geometrical parameters, all the structures share the quasi-planarity of the core porphyrin rings, that are scarcely perturbed by the different substitution modes and show a very small curvature. Yet, a noteworthy structural feature that has to be considered in order to appraise the electronic conjugation between porphyrin and ferrocene systems, is the value of the dihedral angle (torsion) between the carbon atom adjacent to β-pyrrole nitrogen and the carbon atom of the ferrocene cyclopentadienyl ring in the case of the dyad **5t** and **5α** or the carbon atom of the phenyl ring in the case of the dyads **6t** and **6α**. The calculated values are -27.93 (*trans*) and -64.32 (*alpha*) degrees in the couple **5t-5α**, and -25.95 (*trans*) and -59.03 (*alpha*) degrees in the couple **6t-6α**, signalling a progressively deviation from planarity and a consequent smaller conjugation extent.

S5.2. Relative HOMO-LUMO energy levels of the compounds 5*t* and 5α
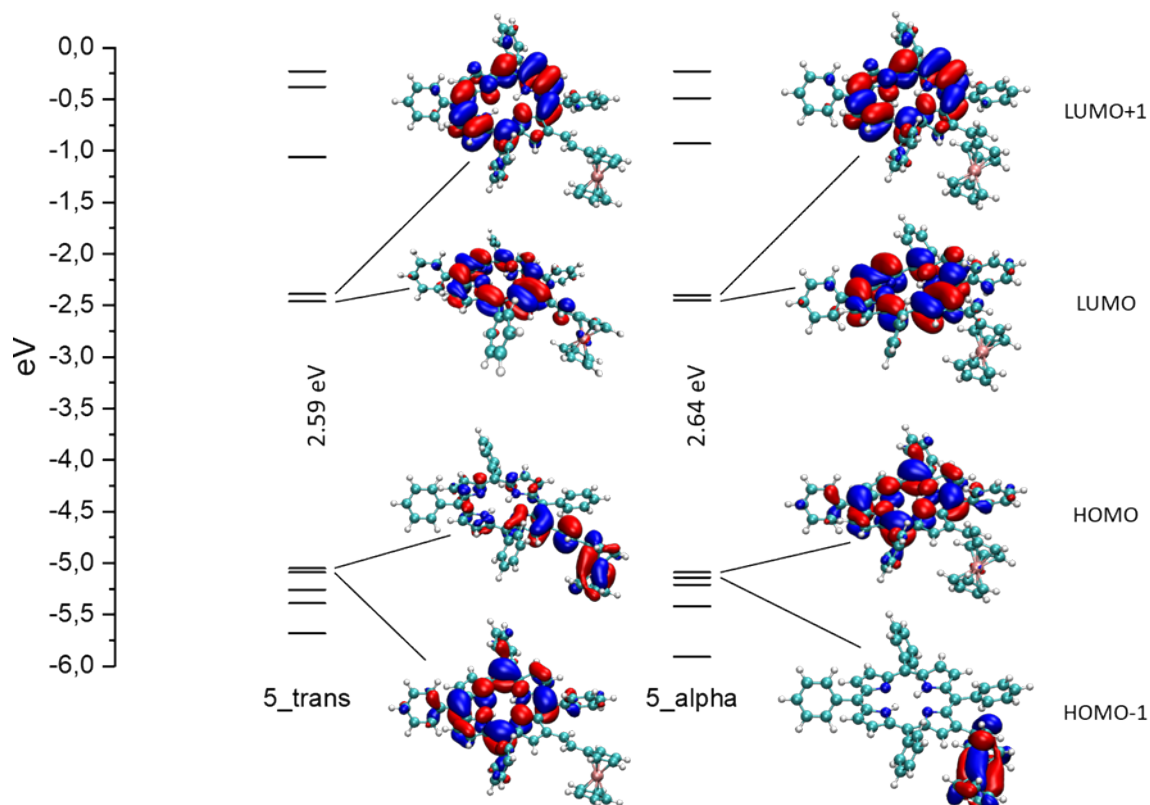
*Fig. S 49 Molecular orbital energy level diagram for trans- (left) and alpha-isomer (right), compounds **5t** and **5α** respectively. calculated with Gaussian16. Band gap (eV) for HOMO-LUMO transition is also reported. Select image of HOMO-1, HOMO, LUMO and LUMO+1 are included to highlight the inversion of the frontier orbital HOMO and HOMO-1 energy level in the two isomers.*

Orbitals	5*t* (trans) E (eV)	5α (alpha) E (eV)
LUMO+1	-2.39	-2.40
LUMO	-2.46	-2.45
HOMO	-5.05	-5.09
HOMO-1	-5.09	-5.14

*Table S 6 Absolute energy (eV) for the first four frontier orbitals of the trans- and alpha-isomers **5t** and **5α**.*

Relative HOMO-LUMO energy levels of the compounds 6t and 6α
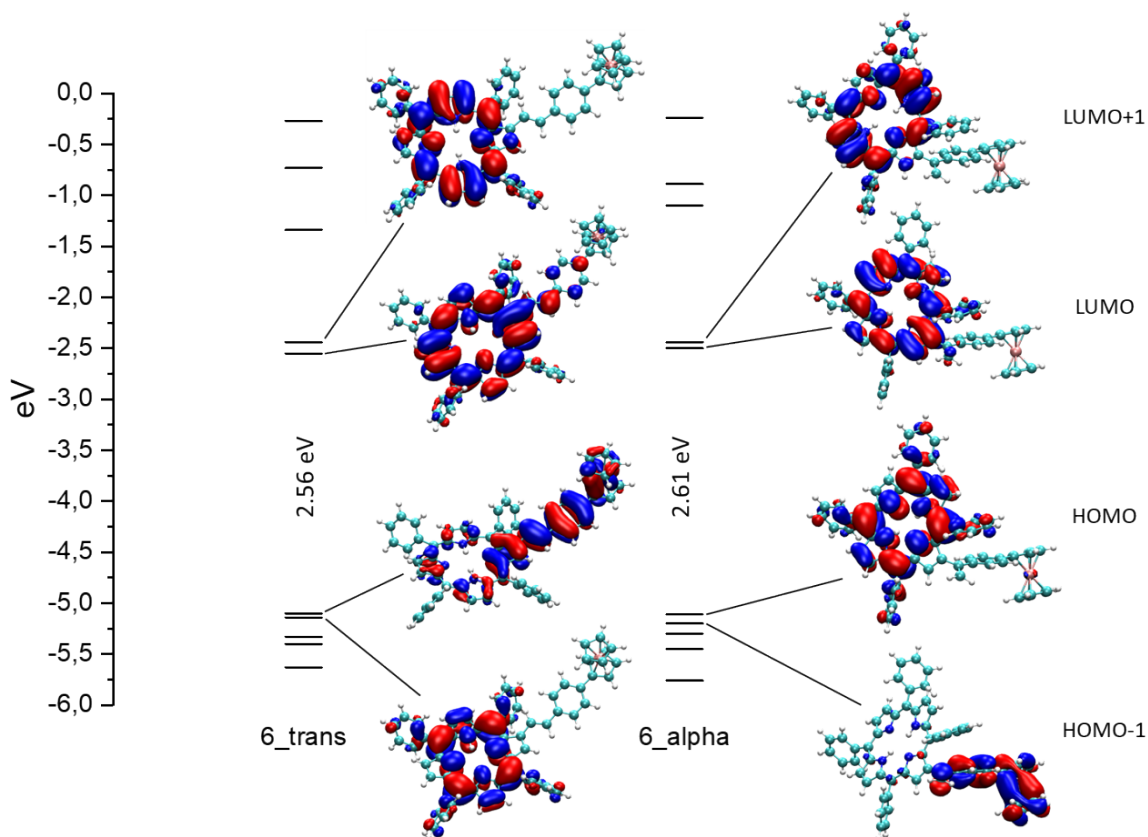
*Fig. S 50 Molecular orbital energy level diagram for trans- (left) and alpha-isomer (right), compounds **6t** and **6α** respectively. calculated with Gaussian16. Band gap (eV) for HOMO-LUMO transition is also reported. Select image of HOMO-1, HOMO, LUMO and LUMO+1 are included to highlight the inversion of the frontier orbital HOMO and HOMO-1 energy level in the two isomers*

Orbitals	**6t** (trans) E (eV)	**6α** (alpha) E (eV)
LUMO+1	-2.44	-2.44
LUMO	-2.55	-2.50
HOMO	-5.10	-5.11
HOMO-1	-5.14	-5.20

*Table S 7 Absolute energy (eV) for the first four frontier orbitals of the trans- and alpha-isomers **6t** and **6α***

References

S1 a) D. Rehm and A. Weller *Isr. J. Chem.* 1970, **8**, 259-271; b) M. Kubo, Y. Mori, M. Otani, M. Murakami, Y. Ishibashi, M. Yasuda, K. Hosomizu,H. Miyasaka, H. Imahori and S. Nakashima *J. Phys. Chem. A*, 2007, **111**, 5136-5143; c) R. Roy, S. Chawla, V. Sharma, A. K. Pal, Y. Silori, A. Datta, A. K. De and A. Lal Koner *Chem. Science*, 2024, **15**, 6363-6377.

S2 M. Taniguchia, J. S. Lindsey, D. F. Bocian and D. Holten *J. Photochem. Photobiol. C_Photochemistry Reviews*, 2021, **46**, 100401.